Learning from Reward-Free Offline Data: A Case for Planning with Latent Dynamics Models

Vlad Sobal[*1] **Wancong Zhang**[*1] **Kynghyun Cho**[1,2] **Randall Balestriero**[3]
Tim G. J. Rudner[4] **Yann LeCun**[1,5]

[1]New York University [2]Genentech [3]Brown University [4]University of Toronto [5]Meta – FAIR

Website Code

Abstract

A long-standing goal in AI is to develop agents capable of solving diverse tasks across a range of environments, including those never seen during training. Two dominant paradigms address this challenge: (i) reinforcement learning (RL), which learns policies via trial and error, and (ii) optimal control, which plans actions using a known or learned dynamics model. However, their comparative strengths in the offline setting—where agents must learn from reward-free trajectories—remain underexplored. In this work, we systematically evaluate RL and control-based methods on a suite of navigation tasks, using offline datasets of varying quality. On the RL side, we consider goal-conditioned and zero-shot methods. On the control side, we train a latent dynamics model using the Joint Embedding Predictive Architecture (JEPA) and employ it for planning. We investigate how factors such as data diversity, trajectory quality, and environment variability influence the performance of these approaches. Our results show that model-free RL benefits most from large amounts of high-quality data, whereas model-based planning generalizes better to unseen layouts and is more data-efficient, while achieving trajectory stitching performance comparable to leading model-free methods. Notably, planning with a latent dynamics model proves to be a strong approach for handling suboptimal offline data and adapting to diverse environments.

1 Introduction

How can we build a system that performs well on unseen combinations of tasks and environments? One promising approach is to avoid relying on online interactions or expert demonstrations, and instead leverage large collections of existing suboptimal trajectories without reward annotations [16, 32, 53]. Broadly, two dominant fields offer promising solutions for learning from such data: reinforcement learning and optimal control.

While online reinforcement learning has enabled agents to master complex tasks—from Atari games [44], Go [60], to controlling real robots [49]—it demands massive quantities of environment interactions. For instance, OpenAI et al. [49] used the equivalent of 100 years of real-time hand manipulation experience to train a robot to reliably handle a Rubik's cube. To address this inefficiency, offline RL methods [18, 33, 41] have been developed to learn behaviors from state–action trajectories with corresponding reward annotations. However, these methods typically train agents for a single task, limiting their reuse in other downstream tasks. To overcome this, recent work has explored learning behaviors from offline reward-free trajectories [32, 52, 53, 67]. This reward-free paradigm is particularly appealing as it allows agents to learn from suboptimal data and use the learned policy to solve a variety of downstream tasks. For example, a system trained on low-quality robotic interactions with cloth can later generalize to tasks like folding laundry [9].

[*] Equal contribution. Author ordering determined by coin flip.

39th Conference on Neural Information Processing Systems (NeurIPS 2025).

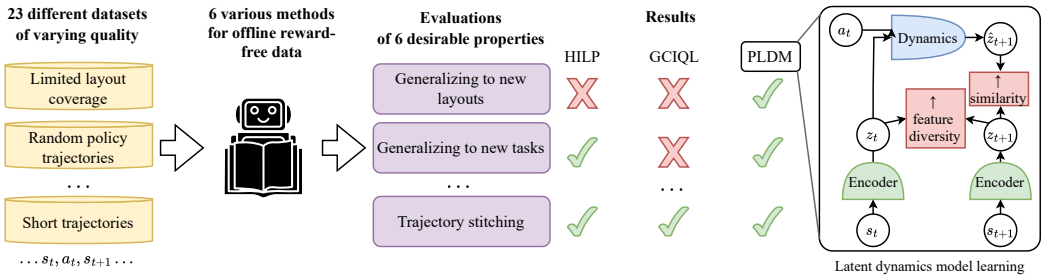

Figure 1: **Overview of our analysis.** We test six methods for learning from offline reward-free trajectories on 23 different datasets across several navigation environments. We evaluate for six generalization properties required to scale to large offline datasets of suboptimal trajectories. We find that planning with a latent dynamics model (PLDM) demonstrates the highest level of generalization. For a full comparison, see Table 1. **Right:** diagram of PLDM. Circles represent variables, rectangles – loss components, half-ovals – trained models.

Optimal control tackles challenge differently: instead of learning a policy function via trial and error, it plans actions using a known dynamics model [7, 63, 64] to plan out actions. Since real-world dynamics are often hard to specify exactly, many approaches instead learn the model from data [20, 71, 77]. This model-based approach has shown generalization in manipulation tasks involving unseen objects [17]. Importantly, dynamics models can be trained directly from reward-free offline trajectories, making this a compelling route [16, 56].

Despite significant advances in RL and optimal control, the role of pre-training data quality on reward-free offline learning remains largely unexplored. Prior work has primarily focused on RL methods trained on data from expert or exploratory policies [22, 76], without isolating the specific aspects of data quality that influence performance. In this work, we address this gap by systematically evaluating the strengths and limitations of various approaches for learning from reward-free trajectories. We assess how different learning paradigms perform under offline datasets that vary in both quality and quantity. To ground our study, we focus on navigation tasks — an essential aspect of many real-world robotic systems — where spatial reasoning, generalization, and trajectory stitching play a critical role. While this choice excludes domains such as manipulation, it offers a controlled yet challenging testbed for our comparative analysis.

Our contributions can be summarized as follows:

1. We propose two new navigation environments with granular control over the data generation process, and generate a total of *23 datasets* of varying quality;
2. We evaluate methods for learning from offline, reward-free trajectories, drawing from both reinforcement learning and optimal control paradigms. Our analysis systematically assesses their ability to learn from random policy trajectories, stitch together short sequences, train effectively on limited data, and generalize to unseen environment layouts and tasks beyond goal-reaching;
3. We demonstrate that learning a latent dynamics model and using it for planning is robust to suboptimal data quality and achieves the highest level of generalization to environment variations;
4. We present a list of guidelines to help practitioners choose between methods depending on available data and generalization requirements.

To facilitate further research into methods for learning from offline trajectories without rewards, we release code, data, environment visualizations, and more at `latent-planning.github.io`.

2 Related Work

Reward-free offline RL refers to learning from offline data that does not contain rewards in a task-agnostic way. The goal is to extract general behaviors from offline data to solve a variety of downstream tasks. One approach uses goal-conditioned RL, with goals sampled in similar manner as in Hindsight Experience Replay [1]. Park et al. [52] show that this can be applied to learn a goal-conditioned policy using IQL, as well as to learn a hierarchical value function. Hatch et al. [29] proposes using a small set of observations corresponding to the solved task to define the task and learn from reward-free data. Hu et al. [30], Yu et al. [79] propose to use labeled data to train a reward function, than label the reward-free trajectories. Zero-shot methods go beyond goal-reaching from

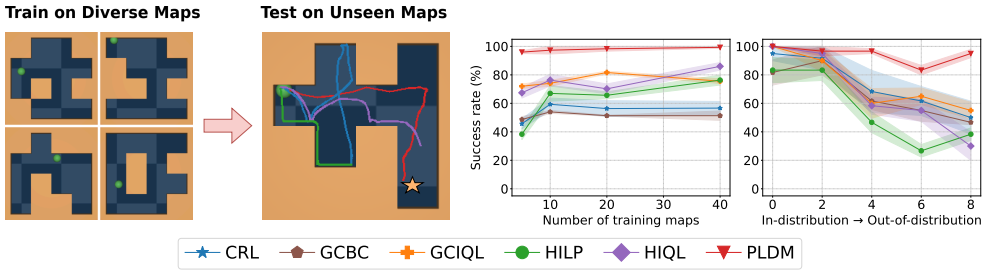

Figure 2: **Left:** We train offline goal-conditioned agents on trajectories collected in a subset of maze layouts (left), and evaluate on held out layouts, observing trajectories shown on the right. Only PLDM solves the task (see Figure 8 for more). **Right:** Success rates of tested methods on held-out layouts, as a function of the number of training layouts. Rightmost plot shows success rates of models trained on data from five layouts, evaluated on held-out layouts ranging from those similar to training layouts to out-of-distribution ones. We use map layout edit distance from the training layouts as a measure of distribution shift. PLDM demonstrates the best generalization performance. Results are averaged over 3 seeds, shaded area denotes standard error. See Figure 1 for more details on PLDM.

offline data and aim to solve arbitrary tasks specified at test time. HILP [53] proposes learning a distance-preserving representation space such that the distance in that space is proportional to the number of steps between two states, similar to Laplacian representations [69, 70, 73]. Forward-Backward representations [67, 68] tackle this with an approach akin to successor-features [5].

Optimal Control, similar to RL, tackles the problem of selecting actions in an environment to optimize a given objective (reward for RL, cost for control). Classical optimal control methods typically assumes that the transition dynamics of the environment are known [7]. This paradigm has been used to control aircraft, rockets, missiles [11] and humanoid robots [35, 57]. When the transition dynamics cannot be defined precisely, they can often be learned [65, 71]. Many RL methods approximate dynamic programming in the context of unknown dynamics [6, 62]. In this work, we use the term RL to refer to methods that either implicitly or explicitly use rewards information to train a policy function, and optimal control for methods that use a dynamics model and explicitly search for actions that optimize the objective.

The importance of offline data has been highlighted in works such as ExORL, [76] which demonstrates that exploratory RL data enables off-policy algorithms to perform well in offline RL; however, it only compares exploratory vs. task-specific data, without analyzing which data aspects affect performance. Buckman et al. [12] investigates the data importance for offline RL with rewards. Recently proposed OGBench [51] introduces multiple offline datasets for a variety of goal-conditioned tasks; in contrast, we conduct a more fine-grained analysis of how methods perform in top-down navigation under suboptimal data conditions and generalize to new tasks and layouts. Yang et al. [74] also study generalization of offline GCRL, but focus on reaching out-of-distribution goals. Ghugare et al. [24] study stitching generalization.

3 The Landscape of Available Methods

In this section, we formally introduce the setting of learning from state-action sequences without reward annotations and overview available approaches. We also introduce a method we call Planning with a Latent Dynamics Model (PLDM).

3.1 Problem Setting

We consider a Markov decision process (MDP) $\mathcal{M} = (\mathcal{S}, \mathcal{A}, \mu, p, r)$, where $\mathcal{S}$ is the state space, $\mathcal{A}$ is the action space, $\mu \in \mathcal{P}(\mathcal{S})$ denotes the initial state distribution, $p \in \mathcal{S} \times \mathcal{A} \to \mathcal{S}$ denotes the transition dynamics (we only consider the deterministic case), and $r \in \mathcal{S} \to \mathbb{R}$ denotes the reward function. We work in the offline setting, where we have access to a dataset of state-action sequences $\mathcal{D}$ which consists of transitions $(s_0, a_0, s_1, \ldots, a_{T-1}, s_T)$. We emphasize again that the offline dataset in our setting does not contain any reward information. The goal is, given $\mathcal{D}$, to find a policy $\pi \in \mathcal{S} \times \mathcal{Z} \to \mathcal{A}$, to maximize cumulative reward r_z, where $\mathcal{Z}$ is the space of possible task definitions. Our goal is to make the best use of the offline dataset $\mathcal{D}$ to enable the agent to

Table 1: **Road-map of our generalization stress-testing experiments.** We test 4 offline goal-conditioned methods - HIQL, GCIQL, CRL, GCBC; a zero-shot RL method HILP, and a learned latent dynamics planning method PLDM. ★★★ denotes good performance in the specified experiment, ★★☆ denotes average performance, and ★☆☆ denotes poor performance. We see that HILP and PLDM are the best-performing methods, with PLDM standing out as the only method that reaches competitive performance in all settings.

Property (Experiment section)	**HILP**	**HIQL**	**GCIQL**	**CRL**	**GCBC**	**PLDM**
Transfer to new environment layouts (4.8)	★☆☆	★☆☆	★☆☆	★☆☆	★☆☆	★★★
Transfer to a new task (4.6)	★★☆	★☆☆	★☆☆	★☆☆	★☆☆	★★★
Data efficiency (4.3)	★☆☆	★★☆	★★★	★★☆	★★☆	★★★
Best-case performance (4.2)	★★★	★★★	★★★	★★★	★★☆	★★★
Can learn from random policy trajectories (4.5)	★★★	★☆☆	★★★	★☆☆	★☆☆	★★☆
Can stitch suboptimal trajectories (4.4)	★★★	★☆☆	★★★	★☆☆	★☆☆	★★☆

solve a variety of tasks in a given environment with potentially different layouts. During evaluation, unless otherwise specified, the agent is tasked to reach a goal state s_g, so the reward is defined as $r_g(s) = \mathbb{I}[s = s_g]$, and $\mathcal{Z}$ is equivalent to $\mathcal{S}$.

3.2 Reward-free Offline Reinforcement Learning

In this work, we study methods that solve tasks purely from offline trajectories without reward annotations. Reward-free offline RL methods fall into two categories: goal-conditioned RL and zero-shot methods that treat the task as a latent variable. We evaluate state-of-the-art methods from both categories on goal-reaching, and test zero-shot methods on their ability to transfer to new tasks. The methods we investigate are:

- **GCIQL** [52] – goal-conditioned version of Implicit Q-Learning [33], a strong and widely-used method for offline RL;
- **HIQL** [52] – a hierarchical GCRL method which trains two policies: one to generate subgoals, and another one to reach the subgoals. Notably, both policies use the same value function;
- **HILP** [53] – a method that learns state representations from the offline data such that the distance in the learned representation space is proportional to the number of steps between two states. A direction-conditioned policy is then learned to be able to move along any specified direction in the latent space;
- **CRL** [19] – uses contrastive learning to learn compatibility between states and possible reachable goals. The learned representation, which has been shown to be directly linked to goal-conditioned Q-function, is then used to train a goal-conditioned policy;
- **GCBC** [23, 43] – Goal-Conditioned Behavior Cloning - the simplest baseline for goal-reaching.

3.3 Planning with a Latent Dynamics Model

The methods in Section 3.2 are model-free, none explicitly model the environment dynamics. Since we do not assume known dynamics as in classical control, we can instead learn a dynamics model from offline data, similar to [46, 55], which propose a model-based method for goal-reaching using an image reconstruction objective.

We propose a model-based method named Planning with a Latent Dynamics Model (PLDM), which learns latent dynamics using a reconstruction-free SSL objective and the JEPA architecture [39]. At test time, we plan in the learned latent space to reach goals. We opt for an SSL approach that predicts the latents as opposed to reconstructing the input observations [3, 21, 26, 81] motivated by findings that reconstruction yields suboptimal features [2, 42], while reconstruction-free representation learning works well for control [27, 59]. Appendix G provides empirical support: features trained with reconstruction-based methods such as DreamerV3 [26] underperform in test-time planning.

Given agent trajectory sequence $(s_0, a_0, s_1, ..., a_{T-1}, s_T)$, we specify the PLDM world model as:

$$\text{Encoder}: \quad \hat{z}_0 = z_0 = h_\theta(s_0) \tag{1}$$

$$\text{Predictors}: \quad \hat{z}_t^k = f_\theta^k(\hat{z}_{t-1}^k, a_{t-1}), \forall k \in \{1, \dots, K\} \tag{2}$$

where $\hat{z}_t^k$ is the latent state predicted by predictor k and z_t is the encoder output at step t. When $K > 1$, we train an ensemble of predictors for uncertainty regularization at test-time. The training objective involves minimizing the distance between predicted and encoded latents summed over

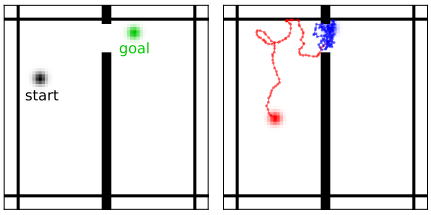

Figure 3: **Left**: The Two-Rooms environment. The agent starts at a random location and is tasked with reaching the goal at another randomly sampled location in the other room using 200 steps or less. Observations are 64×64 pixels images. **Right:** Examples of trajectories in the offline data. Red: each step's direction is sampled from Von Mises distribution. Blue: each step's direction is sampled uniformly.

Table 2: Performance of tested methods on good-quality data and on data with no trajectories passing through the door. Values are average success rates ($\pm$standard error) across 3 seeds.

Method	Good-quality data	No door-passing trajectories
CRL	89.3 ± 0.7	14.7 ± 4.1
GCBC	86.0 ± 2.0	8.4 ± 1.2
GCIQL	98.0 ± 0.9	99.6 ± 0.4
HILP	100.0 ± 0.0	100.0 ± 0.0
HIQL	96.4 ± 1.3	26.3 ± 5.6
PLDM	97.8 ± 0.7	34.4 ± 2.7

all timesteps. Given target and predicted latents $Z, \hat{Z}^k \in \mathbb{R}^{H \times N \times D}$, where $H \leq T$ is the model prediction horizon, N is the batch dimension, and D the feature dimension, the similarity objective between predictions and encodings is:

$$\mathcal{L}_{\text{sim}} = \sum_{k=1}^{K} \sum_{t=0}^{H} \frac{1}{N} \sum_{b=0}^{N} \|\hat{Z}_{t,b}^k - Z_{t,b}\|_2^2 \tag{3}$$

To prevent representation collapse, we use a VICReg-inspired [4] objective, and inverse dynamics modeling [40]. We show a diagram of PLDM in Figure 1. See Appendix D.1.1 for details.

Goal-conditioned planning with PLDM. In this work, we mainly focus on the task of reaching specified goal states. While methods outlined in Section 3.2 rely on trained policies to reach the goal, PLDM relies on planning. At test time, given the current observation s_0, goal observation s_g, pretrained encoder h_θ predictor f_θ, and planning horizon H, our planning objective is:

$$\forall k \in \{1, \dots, K\} : \; \hat{z}_0^k = z_0^k = h_\theta(s_0), \; \hat{z}_t^k = f_\theta^k(\hat{z}_{t-1}^k, a_{t-1}) \tag{4}$$

$$C_{\text{goal}}(\mathbf{a}, s_0, s_g) = \frac{1}{K} \sum_{k=1}^{K} \sum_{t=0}^{H} \|h_\theta(s_g) - f_\theta^k(\hat{z}_t^k, a_t)\| \tag{5}$$

$$C_{\text{uncertainty}}(\mathbf{a}, s_0, s_g) = \sum_{t=0}^{H} \gamma^t \sum_{j=1}^{d} \text{Var}(\{f_{\theta_k}(s_t^k, a_t)_j\}_{k=1}^K) \tag{6}$$

$$\mathbf{a}^* = \arg\min_{\mathbf{a}} \{C_{\text{goal}}(\mathbf{a}, s_0, s_g) + \beta C_{\text{uncertainty}}(\mathbf{a}, s_0, s_g)\} \tag{7}$$

C_{goal} is the goal-reaching objective and $C_{\text{uncertainty}}$ penalizes the model from choosing state-action transitions that deviate from the training distribution, with $\gamma \in [0, 1]$ as the temporal discount. This regularization resembles how GCIQL, HIQL, and HILP use expectile regression to learn policies that remain *in-distribution* with respect to the dataset [34]. See Appendix E for ablations on $C_{\text{uncertainty}}$.

Following the Model Predictive Control framework [45], PLDM re-plans every i interactions with the environment. By default, we use $i = 1$ for all experiments, making PLDM $\sim$ 4x slower than the model-free baselines. The replanning interval i can be increased to accelerate MPC with only a minor loss in performance (see Appendix F). We use MPPI [72] in all our experiments with planning. We note that PLDM is not using rewards, neither explicitly nor implicitly, and should be considered as an optimal control method. We also note that to apply PLDM to a new task, we do not need to retrain the encoder h_θ and dynamics f_θ, we only need to change the cost in Equation (5). We test this flexibility in Section 4.6, where we invert the sign of the cost to make the agent avoid a given state.

4 Every Method Can Excel but Few Generalize

In this section, we conduct thorough experiments testing methods spanning RL and optimal control outlined in Section 3.2 and Section 3.3. We evaluate on navigation tasks where the agent is either a point mass (Section 4.1, Section 4.8) or quadruped (Section 4.7). We generate datasets of varying size and quality and test how a specific data type affects a given method. See Table 1 for overview.

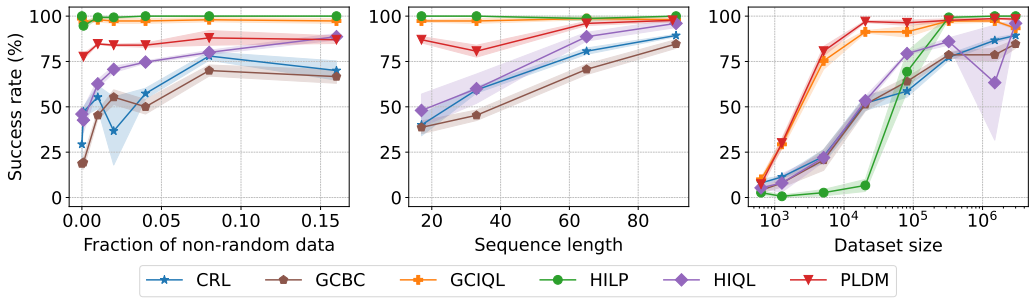

Figure 4: **Testing the selected methods' performance under different dataset constraints.** Values and shaded regions are means and standard error over 3 seeds, respectively. **Left**: To test the importance of the dataset quality, we mix the random policy trajectories with good quality trajectories (see Figure 3). As the amount of good quality data goes to 0, methods begin to fail, with PLDM, GCIQL, and HILP being the most robust ones. **Center**: We measure methods' performance when trained with different sequence lengths. We find that many goal-conditioned methods fail when train trajectories are short, which causes far-away goals to become out-of-distribution for the resulting policy. **Right**: We measure methods' performance with datasets of varying sizes. We see that PLDM and GCIQL are the most sample efficient, and manage to get almost 80% success rate even with a few thousand transitions. See Appendix H for the analysis of statistical significance.

4.1 Two-Rooms Environment

We begin with a navigation task called Two-Rooms, featuring a point-mass agent. Each observation $x_t \in \mathbb{R}^{2\times64\times64}$ is a top-down view: the first channel encodes the agent, the second the walls (Figure 3). Actions $a \in \mathbb{R}^2$ denote the displacement vector of the agent position from one time step to the next, with a norm limit of 2.45. The goal is to reach a randomly sampled state within 200 steps. See Appendix C.2 for more details. This environment allows for controlled data generation – ideal for efficient and thorough experimentation, while still not being too trivial.

Offline data. To generate offline data, we place the agent in a random location within the environment, and execute a sequence of actions for T steps, where T denotes the episode length. The actions are generated by first picking a random direction, then using Von Mises distribution with concentration 5 to sample action directions. The step size is uniform from 0 to 2.45. Unless otherwise specified, the episodes' length is $T = 91$, and the total number of transitions in the data is 3 million.

4.2 What Methods Excel In-Distribution with a Large High-Quality Dataset?

To get the topline performance of the methods under optimal dataset conditions, we test them in a setting with abundant data, good state coverage, and good quality trajectories long enough to traverse the two rooms. With 3 million transitions, corresponding to around 30,000 trajectories, all methods reach good performance in the goal-reaching task in Two-Rooms (Table 2), with HIQL, GCIQL, HILP, and PLDM nearing 100% success rate.

Takeaway: All methods can perform well when data is plentiful and high-quality.

4.3 What Method is the Most Sample-Efficient?

We investigate how different methods perform when the dataset size varies. While our ultimate goal is to have a method that can make use of a large amount of suboptimal offline data, this experiment serves to distinguish which methods can glean the most information from available data. We tried ranges of dataset sizes all the way down to a few thousand transitions. In Figure 4, we see that the model-based PLDM and the model-free GCIQL outperform other model-free methods when data is scarce. In particular, HILP is more data-hungry than other model-free methods but achieves perfect performance with enough data.

Takeaway: PLDM and GCIQL are more sample-efficient than other methods.

4.4 What Methods Can Stitch Suboptimal Trajectories?

Can we learn from short trajectories? We vary the episode length T during data generation to test whether methods can stitch together short training trajectories to reach long-horizon goals. In real-world scenarios, collecting long episodes is often difficult—especially in open-ended environments—so the ability to learn generalizable policies from short trajectories is crucial. The hardest scenario of Two-Rooms requires the agent to navigate from the bottom left corner to the bottom right corner, and involves ~ 90 steps, meaning that with short episode lengths such as 16, the goal is never observed. To succeed, methods must stitch together multiple offline trajectories.

We create datasets with episode length of 91, 64, 32, 16, keeping total transitions number at 3 million. Results in Figure 4 (center) show that with the exception of GCIQL, goal-conditioned model-free methods struggle when trained with shorter episodes. We hypothesize that these methods are limited by dynamic programming on the short transitions, which can be sample-inefficient for stitching many short trajectories to reach far-away goals. In contrast, HILP performs well by learning to follow directions in latent space – even from short episodes. Similarly, PLDM can learn an accurate model from short trajectories and stitch together a plan during test time.

Can we learn from data with imperfect coverage? We artificially constrain trajectories to always stay within one room within the episode, and never pass through the door. Without the constraint, around 35% trajectories pass through the door. During evaluation, the agent still needs to go through the door to reach the goal state. This also reflects possible constraints in real-life scenarios, as the ability to stitch offline trajectories together is essential to efficiently learn from offline data. The results are shown in Table 2. We see that HILP and GCIQL achieve perfect performance, while PLDM performance drops but is still higher than the rest of offline GCRL methods. We hypothesize that HILP's latent space structure enables effective stitching, while PLDM retains some performance due to the learned dynamics. With the exception of GCIQL, other model-free GCRL methods fail to learn to compose trajectories across rooms.

Takeaway: When solving the task requires 'stitching', HILP and GCIQL work great. The performance of PLDM drops, but is better than that of most offline model-free GCRL methods.

4.5 What Methods Can Learn From Trajectories of a Random Policy?

In this experiment, we evaluate how trajectory quality affects agent performance. In practice, random policy data is easy to collect, while expert demonstrations are often unavailable. Thus, algorithms that can generalize from noisy data are crucial. We create a dataset where actions are sampled uniformly at random, causing agents to oscillate near the starting point. In this setting, the average maximum distance between any two points in a trajectory is ~ 10 (when the whole environment is 64 by 64), while when using Von Mises to sample actions as in the case of good quality data, it is ~ 28. Example trajectories from both types of action sampling are shown in Figure 3.

We see that HILP, GCIQL and the model-based PLDM outperform the rest of goal-conditioned RL methods in this setting (Figure 4). We hypothesize that because random trajectories on average do not go far, the sampled state and goal pairs during training are close to each other. As a result, faraway goals become out of distribution, and GCRL methods struggle with long-horizon tasks when TD learning fails to bridge distant trajectories. In contrast, PLDM uses the data only to learn the dynamics model, and random policy trajectories are still suitable for the purpose. HILP learns the latent space and how to traverse it in various dimensions – even from random data.

Takeaway: When the dataset quality is low, HILP, GCIQL and PLDM perform better than other offline GCRL methods.

4.6 What Methods Can Generalize to a New Task?

To build effective general purpose systems that learn from offline data, we need an algorithm that can generalize to different tasks. So far, we evaluated on goal-reaching tasks. In this experiment, we test generalization to a different task in an environment with the same dynamics: avoiding a chasing agent in the same environment. We compare PLDM and HILP, using models trained on optimal data from Section 4.2 without any further training. In this task, the chaser follows an expert policy along the

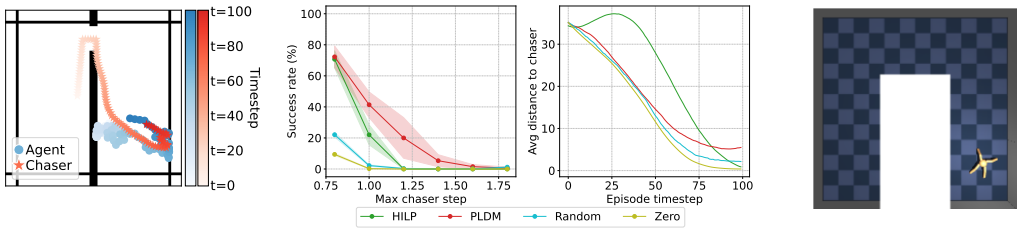

(a) (b) (c)

Figure 5: **Zero-shot generalization to the chasing task. (a)** In the chase environment, the blue agent is tasked with avoiding the red chaser. The chaser follows the shortest path to the agent. The observations of the agent remain unchanged: we pass the chaser state as the goal state. The agent has to avoid the specified state instead of reaching it. **(b) Left**: Performance of the tested methods on the chasing task across different chaser speeds, with faster chaser making the task harder. Baselines include agents that take no action ('Zero') and random actions ('Random'). **(b) Right**: Average distance between the agent and chaser agent throughout the episode when chaser speed is 1.0. **(c)** Visualization of ant-umaze environment. The 4-legged ant is tasked with reaching a randomly sampled goal within a u-shaped room.

shortest path to the agent, and we vary its speed to adjust difficulty. The goal of the controlled agent is to avoid being caught. Goal-conditioned methods are excluded from evaluation, as they cannot avoid specific states by design. At each step, the agent observes the chaser's state and selects actions to maintain distance. In PLDM, we invert the sign of the planning objective to maximize distance in the latent space to the goal state. In HILP, we invert the skill direction. We evaluate the success rate - defined as maintaining a distance ≥ 1.4 pixels over 100 steps. The results are shown in Figure 5b. We also plot average distance between the agents over time in Figure 5b. We see that PLDM performs better than HILP, and is able to evade the chaser more effectively by maintaining greater separation by episode end.

Takeaway: Assuming the environment dynamics remain fixed, PLDM can generalize to tasks other than goal-reaching simply by changing the planning objective.

4.7 Extending to a Higher-Dimensional Control Environment.

So far, we have focused on environments with simple control dynamics over a point-mass agent, where actions are 2D displacement or acceleration vectors. We now investigate whether the same trend holds in a setting with more complex control. We choose Ant-U-Maze, a standard state-based environment with a 29-dimensional state space and 8-dimensional action space (Figure 5c). Solving this task with PLDM requires learning non-trivial dynamics that better resemble real-world control.

We collect a dataset using a pretrained directional expert policy from Park et al. [51], generating 5M transitions by resampling a new direction every 10 steps and adding Gaussian noise with standard deviation 1.0 to each action. For evaluation, the quadruped is initialized at the bottom left or right corner, with the goal at the opposite diagonal. Each method is evaluated on 10 trials.

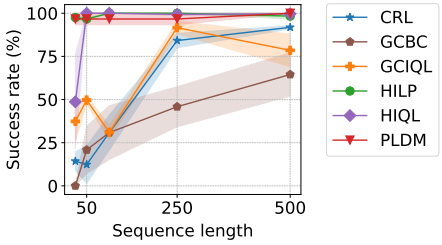

Figure 6: Success rates in Ant-U-Maze for agents trained on trajectories of varying lengths.

As in 4.4, we test the methods' abilities to stitch short training trajectories by using datasets with trajectory lengths 25, 50, 100, 250, and 500 (during evaluation, the start and goal are approximately 200 steps apart). PLDM, HIQL, and HILP outperform other GCRL baselines in trajectory stitching, achieving 100% success rates while other methods fail with shorter trajectories. In contrast to the Two-Rooms experiments, HIQL outperforms GCIQL in this setting. We hypothesize that HIQL's hierarchical structure may particularly benefit high-dimensional ant control: the low-level policy can manage fine-grained joint movements, while the high-level policy can govern overall navigation.

Takeaway: Planning with a latent dynamics model maintains good performance in a standard quadruped maze task, indicating promising generalization to higher control complexity.

4.8 What Methods Can Generalize to Unseen Environment Layouts?

In this experiment, we test whether methods can generalize to new obstacle configurations/layouts – a key requirement for general purpose agents, since collecting data for every scenario is infeasible. We introduce a new navigation environment with slightly more complex dynamics and configurable layouts (Figure 2). Building on top of Mujoco PointMaze, [66] layouts are generated by randomly permuting wall locations. Data is collected by randomly sampling actions at each step. Observation includes an RGB top-down view of the maze and agent velocity; actions are 2D accelerations. The goal is to reach a randomly sampled location. See Appendix C.2 for details.

To test generalization to new obstacle configurations, we vary the number of training maze layouts (5, 10, 20, 40) and evaluate on held-out unseen layouts. For models trained on 5 maps, we further analyze how test-time performance degrades as layouts diverge from the training distribution. Figure 8 shows that PLDM generalizes best – even when trained on just 5 maps – while other methods fail. As test layouts become more out-of-distribution, all methods except PLDM degrade in performance. We also evaluate all methods on a single fixed layout and observe 100% success rate across the board (Table 4). Figure 7 and 8 show PLDM's inferred plans and trajectories from different agents. We also investigate HILP's failure to generalize in Appendix I, and show that HILP's learned representation space successfully captures distance between states in mazes seen during training, but fails on unseen mazes.

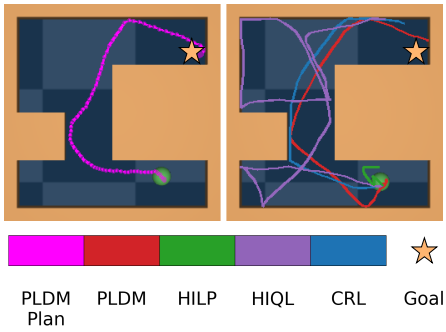

Figure 7: **Left**: Plans generated by PLDM at test time. **Right**: Actual agent trajectories for the tested methods. PLDM is the only method that reliably succeeds on held-out mazes.

Takeaway: The model-based approach enables better generalization to unseen obstacle layouts than model-free methods.

5 Conclusion

In this work, we conducted a comprehensive study of existing methods for learning from offline data without rewards, spanning both reinforcement learning and optimal control, aiming to identify the most promising approaches for leveraging suboptimal trajectories. We focus on a set of navigation tasks that present unique challenges due to the need for spatial reasoning, generalization to new layouts, and trajectory stitching. Our findings highlight HILP and PLDM as the strongest candidates, with PLDM demonstrating the best generalization to new obstacle layouts and to a state-avoidance task. We aggregate our experimental results in Table 1. Overall, we draw three main conclusions:

1. PLDM exhibits robustness to data quality, a high level of data efficiency, best-of-class generalization to new layouts, and excels at adapting to tasks beyond goal-reaching;
2. Learning a well-structured latent-space (e.g. using HILP) enables trajectory stitching and robustness to data quality, although it is more data-hungry than other methods;
3. Model-free GCRL methods are a great choice when the data is plentiful and good quality.

Future work. Our findings indicate that learning and planning with latent dynamics models is a promising direction for building general autonomous agents. There are many promising areas for exploration: 1) extending PLDM to more complex domains such as robotic manipulation and partially observable environments; 2) investigating improved dynamics learning methods to mitigate issues like accumulating prediction errors for tasks involving long-horizon reasoning [37]; and 3) improving test-time efficiency, either by backpropagating gradients through the forward model [8] or via amortized planning.

Acknowledgments

This work was supported through the NYU IT High Performance Computing resources, services, and staff expertise, by the Institute of Information & Communications Technology Planning & Evaluation (IITP) with a grant funded by the Ministry of Science and ICT (MSIT) of the Republic of Korea in connection with the Global AI Frontier Lab International Collaborative Research, by the Samsung Advanced Institute of Technology (under the project Next Generation Deep Learning: From Pattern Recognition to AI) and the National Science Foundation (under NSF Award 1922658), and in part by AFOSR grant FA9550-23-1-0139 "World Models and Autonomous Machine Intelligence" and by ONR MURI N00014-22-1-2773 "Self-Learning Perception through Interaction with the Real World".

References

[1] M. Andrychowicz, F. Wolski, A. Ray, J. Schneider, R. Fong, P. Welinder, B. McGrew, J. Tobin, O. Pieter Abbeel, and W. Zaremba. Hindsight experience replay. *Advances in neural information processing systems*, 30, 2017.

[2] R. Balestriero and Y. LeCun. Learning by reconstruction produces uninformative features for perception. *arXiv preprint arXiv:2402.11337*, 2024.

[3] E. Banijamali, R. Shu, M. Ghavamzadeh, H. Bui, and A. Ghodsi. Robust locally-linear controllable embedding. (arXiv:1710.05373), Feb. 2018. doi: 10.48550/arXiv.1710.05373. URL http://arxiv.org/abs/1710.05373. arXiv:1710.05373 [cs].

[4] A. Bardes, J. Ponce, and Y. LeCun. Vicreg: Variance-invariance-covariance regularization for self-supervised learning. *arXiv preprint arXiv:2105.04906*, 2021.

[5] A. Barreto, W. Dabney, R. Munos, J. J. Hunt, T. Schaul, H. P. van Hasselt, and D. Silver. Successor features for transfer in reinforcement learning. *Advances in neural information processing systems*, 30, 2017.

[6] D. Bertsekas. *Dynamic programming and optimal control: Volume I*, volume 4. Athena scientific, 2012.

[7] D. P. Bertsekas. *Reinforcement Learning and Optimal Control*. Athena Scientific, Belmont, MA, 2019. ISBN 978-1-886529-46-6. URL https://www.mit.edu/~dimitrib/RLbook.html.

[8] H. Bharadhwaj, K. Xie, and F. Shkurti. Model-predictive control via cross-entropy and gradient-based optimization. In *Learning for Dynamics and Control*, pages 277–286. PMLR, 2020.

[9] K. Black, N. Brown, D. Driess, A. Esmail, M. Equi, C. Finn, N. Fusai, L. Groom, K. Hausman, B. Ichter, et al. π_0: A vision-language-action flow model for general robot control. *arXiv preprint arXiv:2410.24164*, 2024.

[10] A. Brohan, N. Brown, J. Carbajal, Y. Chebotar, X. Chen, K. Choromanski, T. Ding, D. Driess, A. Dubey, C. Finn, et al. Rt-2: Vision-language-action models transfer web knowledge to robotic control. *arXiv preprint arXiv:2307.15818*, 2023.

[11] A. E. Bryson. Optimal control-1950 to 1985. *IEEE Control Systems Magazine*, 16(3):26–33, 1996.

[12] J. Buckman, C. Gelada, and M. G. Bellemare. The importance of pessimism in fixed-dataset policy optimization. *arXiv preprint arXiv:2009.06799*, 2020.

[13] M. Caron, H. Touvron, I. Misra, H. Jégou, J. Mairal, P. Bojanowski, and A. Joulin. Emerging properties in self-supervised vision transformers. In *Proceedings of the IEEE/CVF international conference on computer vision*, pages 9650–9660, 2021.

[14] K. Cho. On the properties of neural machine translation: Encoder-decoder approaches. *arXiv preprint arXiv:1409.1259*, 2014.

[15] O. X.-E. Collaboration, A. O'Neill, A. Rehman, A. Gupta, A. Maddukuri, A. Gupta, A. Padalkar, A. Lee, A. Pooley, A. Gupta, A. Mandlekar, A. Jain, A. Tung, A. Bewley, A. Herzog, A. Irpan, A. Khazatsky, A. Rai, A. Gupta, A. Wang, A. Kolobov, A. Singh, A. Garg, A. Kembhavi, A. Xie, A. Brohan, A. Raffin, A. Sharma, A. Yavary, A. Jain, A. Balakrishna, A. Wahid, B. Burgess-Limerick, B. Kim, B. Schölkopf, B. Wulfe, B. Ichter, C. Lu, C. Xu, C. Le, C. Finn, C. Wang, C. Xu, C. Chi, C. Huang, C. Chan, C. Agia, C. Pan, C. Fu, C. Devin, D. Xu, D. Morton, D. Driess, D. Chen, D. Pathak, D. Shah, D. Büchler, D. Jayaraman, D. Kalashnikov, D. Sadigh, E. Johns, E. Foster, F. Liu, F. Ceola, F. Xia, F. Zhao, F. V. Frujeri, F. Stulp, G. Zhou, G. S. Sukhatme, G. Salhotra, G. Yan, G. Feng, G. Schiavi, G. Berseth, G. Kahn, G. Yang, G. Wang, H. Su, H.-S. Fang, H. Shi, H. Bao, H. B. Amor, H. I. Christensen, H. Furuta, H. Bharadhwaj, H. Walke, H. Fang, H. Ha, I. Mordatch, I. Radosavovic, I. Leal, J. Liang, J. Abou-Chakra, J. Kim, J. Drake, J. Peters, J. Schneider, J. Hsu, J. Vakil, J. Bohg, J. Bingham, J. Wu, J. Gao, J. Hu, J. Wu, J. Wu, J. Sun, J. Luo, J. Gu, J. Tan, J. Oh, J. Wu, J. Lu, J. Yang, J. Malik, J. Silvério, J. Hejna, J. Booher, J. Tompson, J. Yang, J. Salvador, J. J. Lim, J. Han, K. Wang, K. Rao, K. Pertsch, K. Hausman, K. Go, K. Gopalakrishnan, K. Goldberg, K. Byrne, K. Oslund, K. Kawaharazuka, K. Black, K. Lin, K. Zhang, K. Ehsani, K. Lekkala, K. Ellis, K. Rana, K. Srinivasan, K. Fang, K. P. Singh, K.-H. Zeng, K. Hatch, K. Hsu, L. Itti, L. Y. Chen, L. Pinto, L. Fei-Fei, L. Tan, L. J. Fan, L. Ott, L. Lee, L. Weihs, M. Chen, M. Lepert, M. Memmel, M. Tomizuka, M. Itkina, M. G. Castro, M. Spero, M. Du, M. Ahn, M. C. Yip, M. Zhang, M. Ding, M. Heo, M. K. Srirama, M. Sharma, M. J. Kim, M. Z. Irshad, N. Kanazawa, N. Hansen, N. Heess, N. J. Joshi, N. Suenderhauf, N. Liu, N. D. Palo, N. M. M. Shafiullah, O. Mees, O. Kroemer, O. Bastani, P. R. Sanketi, P. T. Miller, P. Yin, P. Wohlhart, P. Xu, P. D. Fagan, P. Mitrano, P. Sermanet, P. Abbeel, P. Sundaresan, Q. Chen, Q. Vuong, R. Rafailov, R. Tian, R. Doshi, R. Mart'in-Mart'in, R. Baijal, R. Scalise, R. Hendrix, R. Lin, R. Qian, R. Zhang, R. Mendonca, R. Shah, R. Hoque, R. Julian, S. Bustamante, S. Kirmani, S. Levine, S. Lin, S. Moore, S. Bahl, S. Dass, S. Sonawani, S. Tulsiani, S. Song, S. Xu, S. Haldar, S. Karamcheti, S. Adebola, S. Guist, S. Nasiriany, S. Schaal, S. Welker, S. Tian, S. Ramamoorthy, S. Dasari, S. Belkhale, S. Park, S. Nair, S. Mirchandani, T. Osa, T. Gupta, T. Harada, T. Matsushima, T. Xiao, T. Kollar, T. Yu, T. Ding, T. Davchev, T. Z. Zhao, T. Armstrong, T. Darrell, T. Chung, V. Jain, V. Kumar, V. Vanhoucke, V. Guizilini, W. Zhan, W. Zhou, W. Burgard, X. Chen, X. Chen, X. Wang, X. Zhu, X. Geng, X. Liu, X. Liangwei, X. Li, Y. Pang, Y. Lu, Y. J. Ma, Y. Kim, Y. Chebotar, Y. Zhou, Y. Zhu, Y. Wu, Y. Xu, Y. Wang, Y. Bisk, Y. Dou, Y. Cho, Y. Lee, Y. Cui, Y. Cao, Y.-H. Wu, Y. Tang, Y. Zhu, Y. Zhang, Y. Jiang, Y. Li, Y. Li, Y. Iwasawa, Y. Matsuo, Z. Ma, Z. Xu, Z. J. Cui, Z. Zhang, Z. Fu, and Z. Lin. Open X-Embodiment: Robotic learning datasets and RT-X models. https://arxiv.org/abs/2310.08864, 2023.

[16] S. Dasari, F. Ebert, S. Tian, S. Nair, B. Bucher, K. Schmeckpeper, S. Singh, S. Levine, and C. Finn. Robonet: Large-scale multi-robot learning. (arXiv:1910.11215), Jan. 2020. doi: 10.48550/arXiv.1910.11215. URL http://arxiv.org/abs/1910.11215. arXiv:1910.11215 [cs].

[17] F. Ebert, C. Finn, S. Dasari, A. Xie, A. Lee, and S. Levine. Visual foresight: Model-based deep reinforcement learning for vision-based robotic control. (arXiv:1812.00568), Dec. 2018. doi: 10.48550/arXiv.1812.00568. URL http://arxiv.org/abs/1812.00568. arXiv:1812.00568 [cs].

[18] D. Ernst, P. Geurts, and L. Wehenkel. Tree-based batch mode reinforcement learning. *Journal of Machine Learning Research*, 6, 2005.

[19] B. Eysenbach, T. Zhang, S. Levine, and R. R. Salakhutdinov. Contrastive learning as goal-conditioned reinforcement learning. *Advances in Neural Information Processing Systems*, 35: 35603–35620, 2022.

[20] C. Finn and S. Levine. Deep visual foresight for planning robot motion. (arXiv:1610.00696), Mar. 2017. doi: 10.48550/arXiv.1610.00696. URL http://arxiv.org/abs/1610.00696. arXiv:1610.00696 [cs].

[21] C. Finn, X. Y. Tan, Y. Duan, T. Darrell, S. Levine, and P. Abbeel. Deep spatial autoencoders for visuomotor learning. (arXiv:1509.06113), Mar. 2016. doi: 10.48550/arXiv.1509.06113. URL http://arxiv.org/abs/1509.06113. arXiv:1509.06113 [cs].

[22] J. Fu, A. Kumar, O. Nachum, G. Tucker, and S. Levine. D4rl: Datasets for deep data-driven reinforcement learning. *arXiv preprint arXiv:2004.07219*, 2020.

[23] D. Ghosh, A. Gupta, A. Reddy, J. Fu, C. Devin, B. Eysenbach, and S. Levine. Learning to reach goals via iterated supervised learning. *arXiv preprint arXiv:1912.06088*, 2019.

[24] R. Ghugare, M. Geist, G. Berseth, and B. Eysenbach. Closing the gap between td learning and supervised learning–a generalisation point of view. *arXiv preprint arXiv:2401.11237*, 2024.

[25] D. Hafner, T. Lillicrap, I. Fischer, R. Villegas, D. Ha, H. Lee, and J. Davidson. Learning latent 423 dynamics for planning from pixels. *arXiv preprint arXiv:1811.04551*, 424, 2018.

[26] D. Hafner, J. Pasukonis, J. Ba, and T. Lillicrap. Mastering diverse domains through world models. *arXiv preprint arXiv:2301.04104*, 2023.

[27] N. Hansen, X. Wang, and H. Su. Temporal difference learning for model predictive control. *arXiv preprint arXiv:2203.04955*, 2022.

[28] N. Hansen, H. Su, and X. Wang. Td-mpc2: Scalable, robust world models for continuous control. *arXiv preprint arXiv:2310.16828*, 2023.

[29] K. Hatch, T. Yu, R. Rafailov, and C. Finn. Example-based offline reinforcement learning without rewards. *Proceedings of Machine Learning Research vol*, 144:1–17, 2022.

[30] H. Hu, Y. Yang, Q. Zhao, and C. Zhang. The provable benefits of unsupervised data sharing for offline reinforcement learning. *arXiv preprint arXiv:2302.13493*, 2023.

[31] A. Khazatsky, K. Pertsch, S. Nair, A. Balakrishna, S. Dasari, S. Karamcheti, S. Nasiriany, M. K. Srirama, L. Y. Chen, K. Ellis, P. D. Fagan, J. Hejna, M. Itkina, M. Lepert, Y. J. Ma, P. T. Miller, J. Wu, S. Belkhale, S. Dass, H. Ha, A. Jain, A. Lee, Y. Lee, M. Memmel, S. Park, I. Radosavovic, K. Wang, A. Zhan, K. Black, C. Chi, K. B. Hatch, S. Lin, J. Lu, J. Mercat, A. Rehman, P. R. Sanketi, A. Sharma, C. Simpson, Q. Vuong, H. R. Walke, B. Wulfe, T. Xiao, J. H. Yang, A. Yavary, T. Z. Zhao, C. Agia, R. Baijal, M. G. Castro, D. Chen, Q. Chen, T. Chung, J. Drake, E. P. Foster, J. Gao, D. A. Herrera, M. Heo, K. Hsu, J. Hu, D. Jackson, C. Le, Y. Li, K. Lin, R. Lin, Z. Ma, A. Maddukuri, S. Mirchandani, D. Morton, T. Nguyen, A. O'Neill, R. Scalise, D. Seale, V. Son, S. Tian, E. Tran, A. E. Wang, Y. Wu, A. Xie, J. Yang, P. Yin, Y. Zhang, O. Bastani, G. Berseth, J. Bohg, K. Goldberg, A. Gupta, A. Gupta, D. Jayaraman, J. J. Lim, J. Malik, R. Martín-Martín, S. Ramamoorthy, D. Sadigh, S. Song, J. Wu, M. C. Yip, Y. Zhu, T. Kollar, S. Levine, and C. Finn. Droid: A large-scale in-the-wild robot manipulation dataset. 2024.

[32] J. Kim, S. Park, and S. Levine. Unsupervised-to-online reinforcement learning. *arXiv preprint arXiv:2408.14785*, 2024.

[33] I. Kostrikov, A. Nair, and S. Levine. Offline reinforcement learning with implicit q-learning. *arXiv preprint arXiv:2110.06169*, 2021.

[34] I. Kostrikov, A. Nair, and S. Levine. Offline reinforcement learning with implicit q-learning. In *International Conference on Learning Representations*, 2022. URL https://arxiv.org/abs/2110.06169.

[35] S. Kuindersma, R. Deits, M. Fallon, A. Valenzuela, H. Dai, F. Permenter, T. Koolen, P. Marion, and R. Tedrake. Optimization-based locomotion planning, estimation, and control design for the atlas humanoid robot. *Autonomous robots*, 40:429–455, 2016.

[36] A. Kumar, A. Zhou, G. Tucker, and S. Levine. Conservative q-learning for offline reinforcement learning. In *Advances in Neural Information Processing Systems*, volume 33, pages 1179–1191, 2020. URL https://arxiv.org/abs/2006.04779.

[37] N. Lambert, K. Pister, and R. Calandra. Investigating compounding prediction errors in learned dynamics models. (arXiv:2203.09637), Mar. 2022. doi: 10.48550/arXiv.2203.09637. URL http://arxiv.org/abs/2203.09637. arXiv:2203.09637 [cs].

[38] M. Laskin, A. Srinivas, and P. Abbeel. Curl: Contrastive unsupervised representations for reinforcement learning. In *International conference on machine learning*, pages 5639–5650. PMLR, 2020.

[39] Y. LeCun. A path towards autonomous machine intelligence version 0.9. 2, 2022-06-27. *Open Review*, 62(1):1–62, 2022.

[40] T. Lesort, N. Díaz-Rodríguez, J.-F. Goudou, and D. Filliat. State representation learning for control: An overview. *Neural Networks*, 108:379–392, 2018.

[41] S. Levine, A. Kumar, G. Tucker, and J. Fu. Offline reinforcement learning: Tutorial, review, and perspectives on open problems. *arXiv preprint arXiv:2005.01643*, 2020.

[42] E. Littwin, O. Saremi, M. Advani, V. Thilak, P. Nakkiran, C. Huang, and J. Susskind. How jepa avoids noisy features: The implicit bias of deep linear self distillation networks. *arXiv preprint arXiv:2407.03475*, 2024.

[43] C. Lynch, M. Khansari, T. Xiao, V. Kumar, J. Tompson, S. Levine, and P. Sermanet. Learning latent plans from play. In *Conference on robot learning*, pages 1113–1132. PMLR, 2020.

[44] V. Mnih. Playing atari with deep reinforcement learning. *arXiv preprint arXiv:1312.5602*, 2013.

[45] M. Morari and J. H. Lee. Model predictive control: past, present and future. *Computers & chemical engineering*, 23(4-5):667–682, 1999.

[46] S. Nair, S. Savarese, and C. Finn. Goal-aware prediction: Learning to model what matters. In *International Conference on Machine Learning*, pages 7207–7219. PMLR, 2020.

[47] S. Nair, A. Rajeswaran, V. Kumar, C. Finn, and A. Gupta. R3m: A universal visual representation for robot manipulation. *arXiv preprint arXiv:2203.12601*, 2022.

[48] Octo Model Team, D. Ghosh, H. Walke, K. Pertsch, K. Black, O. Mees, S. Dasari, J. Hejna, C. Xu, J. Luo, T. Kreiman, Y. Tan, L. Y. Chen, P. Sanketi, Q. Vuong, T. Xiao, D. Sadigh, C. Finn, and S. Levine. Octo: An open-source generalist robot policy. In *Proceedings of Robotics: Science and Systems*, Delft, Netherlands, 2024.

[49] M. A. OpenAI, B. Baker, M. Chociej, R. Józefowicz, B. McGrew, J. W. Pachocki, J. Pachocki, A. Petron, M. Plappert, G. Powell, et al. Learning dexterous in-hand manipulation. corr abs/1808.00177 (2018). *arXiv preprint arXiv:1808.00177*, 2018.

[50] M. Oquab, T. Darcet, T. Moutakanni, H. Vo, M. Szafraniec, V. Khalidov, P. Fernandez, D. Haziza, F. Massa, A. El-Nouby, et al. Dinov2: Learning robust visual features without supervision. *arXiv preprint arXiv:2304.07193*, 2023.

[51] S. Park, K. Frans, B. Eysenbach, and S. Levine. Ogbench: Benchmarking offline goal-conditioned rl. *arXiv preprint arXiv:2410.20092*, 2024.

[52] S. Park, D. Ghosh, B. Eysenbach, and S. Levine. Hiql: Offline goal-conditioned rl with latent states as actions. *Advances in Neural Information Processing Systems*, 36, 2024.

[53] S. Park, T. Kreiman, and S. Levine. Foundation policies with hilbert representations. *arXiv preprint arXiv:2402.15567*, 2024.

[54] A. Paszke, S. Gross, F. Massa, A. Lerer, J. Bradbury, G. Chanan, T. Killeen, Z. Lin, N. Gimelshein, L. Antiga, et al. Pytorch: An imperative style, high-performance deep learning library. *Advances in neural information processing systems*, 32, 2019.

[55] K. Pertsch, O. Rybkin, F. Ebert, S. Zhou, D. Jayaraman, C. Finn, and S. Levine. Long-horizon visual planning with goal-conditioned hierarchical predictors. *Advances in Neural Information Processing Systems*, 33:17321–17333, 2020.

[56] O. Rybkin, K. Pertsch, K. G. Derpanis, K. Daniilidis, and A. Jaegle. Learning what you can do before doing anything. *arXiv preprint arXiv:1806.09655*, 2018.

[57] G. Schultz and K. Mombaur. Modeling and optimal control of human-like running. *IEEE/ASME Transactions on mechatronics*, 15(5):783–792, 2009.

[58] M. Schwarzer, N. Rajkumar, M. Noukhovitch, A. Anand, L. Charlin, R. D. Hjelm, P. Bachman, and A. C. Courville. Pretraining representations for data-efficient reinforcement learning. *Advances in Neural Information Processing Systems*, 34:12686–12699, 2021.

[59] R. Shu, T. Nguyen, Y. Chow, T. Pham, K. Than, M. Ghavamzadeh, S. Ermon, and H. H. Bui. Predictive coding for locally-linear control. (arXiv:2003.01086), Mar. 2020. doi: 10.48550/arXiv.2003.01086. URL http://arxiv.org/abs/2003.01086. arXiv:2003.01086 [cs].

[60] D. Silver, A. Huang, C. J. Maddison, A. Guez, L. Sifre, G. Van Den Driessche, J. Schrittwieser, I. Antonoglou, V. Panneershelvam, M. Lanctot, et al. Mastering the game of go with deep neural networks and tree search. *nature*, 529(7587):484–489, 2016.

[61] V. Sobal, J. SV, S. Jalagam, N. Carion, K. Cho, and Y. LeCun. Joint embedding predictive architectures focus on slow features. *arXiv preprint arXiv:2211.10831*, 2022.

[62] R. S. Sutton. Reinforcement learning: An introduction. *A Bradford Book*, 2018.

[63] Y. Tassa, T. Erez, and W. Smart. Receding horizon differential dynamic programming. In J. Platt, D. Koller, Y. Singer, and S. Roweis, editors, *Advances in Neural Information Processing Systems*, volume 20. Curran Associates, Inc., 2007. URL https://proceedings.neurips.cc/paper_files/paper/2007/file/c6bff625bdb0393992c9d4db0c6bbe45-Paper.pdf.

[64] E. Todorov and W. Li. A generalized iterative lqg method for locally-optimal feedback control of constrained nonlinear stochastic systems. In *Proceedings of the 2005, American Control Conference, 2005.*, pages 300–306 vol. 1, 2005. doi: 10.1109/ACC.2005.1469949.

[65] E. Todorov and W. Li. A generalized iterative lqg method for locally-optimal feedback control of constrained nonlinear stochastic systems. In *Proceedings of the 2005, American Control Conference, 2005.*, pages 300–306. IEEE, 2005.

[66] E. Todorov, T. Erez, and Y. Tassa. Mujoco: A physics engine for model-based control. In *IROS*, pages 5026–5033. IEEE, 2012. ISBN 978-1-4673-1737-5. URL http://dblp.uni-trier.de/db/conf/iros/iros2012.html#TodorovET12.

[67] A. Touati and Y. Ollivier. Learning one representation to optimize all rewards. *Advances in Neural Information Processing Systems*, 34:13–23, 2021.

[68] A. Touati, J. Rapin, and Y. Ollivier. Does zero-shot reinforcement learning exist? *arXiv preprint arXiv:2209.14935*, 2022.

[69] K. Wang, K. Zhou, Q. Zhang, J. Shao, B. Hooi, and J. Feng. Towards better laplacian representation in reinforcement learning with generalized graph drawing. In *International Conference on Machine Learning*, pages 11003–11012. PMLR, 2021.

[70] K. Wang, K. Zhou, J. Feng, B. Hooi, and X. Wang. Reachability-aware laplacian representation in reinforcement learning. *arXiv preprint arXiv:2210.13153*, 2022.

[71] M. Watter, J. T. Springenberg, J. Boedecker, and M. Riedmiller. Embed to control: A locally linear latent dynamics model for control from raw images. (arXiv:1506.07365), Nov. 2015. doi: 10.48550/arXiv.1506.07365. URL http://arxiv.org/abs/1506.07365. arXiv:1506.07365 [cs].

[72] G. Williams, A. Aldrich, and E. Theodorou. Model predictive path integral control using covariance variable importance sampling. *arXiv preprint arXiv:1509.01149*, 2015.

[73] Y. Wu, G. Tucker, and O. Nachum. The laplacian in rl: Learning representations with efficient approximations. *arXiv preprint arXiv:1810.04586*, 2018.

[74] R. Yang, L. Yong, X. Ma, H. Hu, C. Zhang, and T. Zhang. What is essential for unseen goal generalization of offline goal-conditioned rl? In *International Conference on Machine Learning*, pages 39543–39571. PMLR, 2023.

[75] S. Yang, O. Nachum, Y. Du, J. Wei, P. Abbeel, and D. Schuurmans. Foundation models for decision making: Problems, methods, and opportunities. *arXiv preprint arXiv:2303.04129*, 2023.

[76] D. Yarats, D. Brandfonbrener, H. Liu, M. Laskin, P. Abbeel, A. Lazaric, and L. Pinto. Don't change the algorithm, change the data: Exploratory data for offline reinforcement learning. *arXiv preprint arXiv:2201.13425*, 2022.

[77] L. Yen-Chen, M. Bauza, and P. Isola. Experience-embedded visual foresight. (arXiv:1911.05071), Nov. 2019. doi: 10.48550/arXiv.1911.05071. URL http://arxiv.org/abs/1911.05071. arXiv:1911.05071 [cs].

[78] T. Yu, G. Thomas, L. Yu, T. X. Ma, S. Ermon, J. Zou, and C. Finn. Mopo: Model-based offline policy optimization. *Advances in Neural Information Processing Systems*, 33:14129–14142, 2020. URL https://arxiv.org/abs/2005.13239.

[79] T. Yu, A. Kumar, Y. Chebotar, K. Hausman, C. Finn, and S. Levine. How to leverage unlabeled data in offline reinforcement learning. In *International Conference on Machine Learning*, pages 25611–25635. PMLR, 2022.

[80] M. Zare, P. M. Kebria, A. Khosravi, and S. Nahavandi. A survey of imitation learning: Algorithms, recent developments, and challenges. *IEEE Transactions on Cybernetics*, 2024.

[81] M. Zhang, S. Vikram, L. Smith, P. Abbeel, M. J. Johnson, and S. Levine. Solar: Deep structured representations for model-based reinforcement learning. (arXiv:1808.09105), June 2019. doi: 10.48550/arXiv.1808.09105. URL http://arxiv.org/abs/1808.09105. arXiv:1808.09105 [cs].

[82] W. Zhang, A. GX-Chen, V. Sobal, Y. LeCun, and N. Carion. Light-weight probing of unsupervised representations for reinforcement learning. *arXiv preprint arXiv:2208.12345*, 2022.

[83] G. Zhou, H. Pan, Y. LeCun, and L. Pinto. Dino-wm: World models on pre-trained visual features enable zero-shot planning. *arXiv preprint arXiv:2411.04983*, 2024.

Appendix

Table of Contents

A Reproducibility

Code is available at https://github.com/vladisai/PLDM

An implementation of our method is provided in the GitHub repository above, which includes environments, data generation, training, and evaluation scripts. Detailed hyperparameters for our method and the baselines are provided in Appendix J.

B Visualization of Plans and Trajectories for Diverse PointMaze

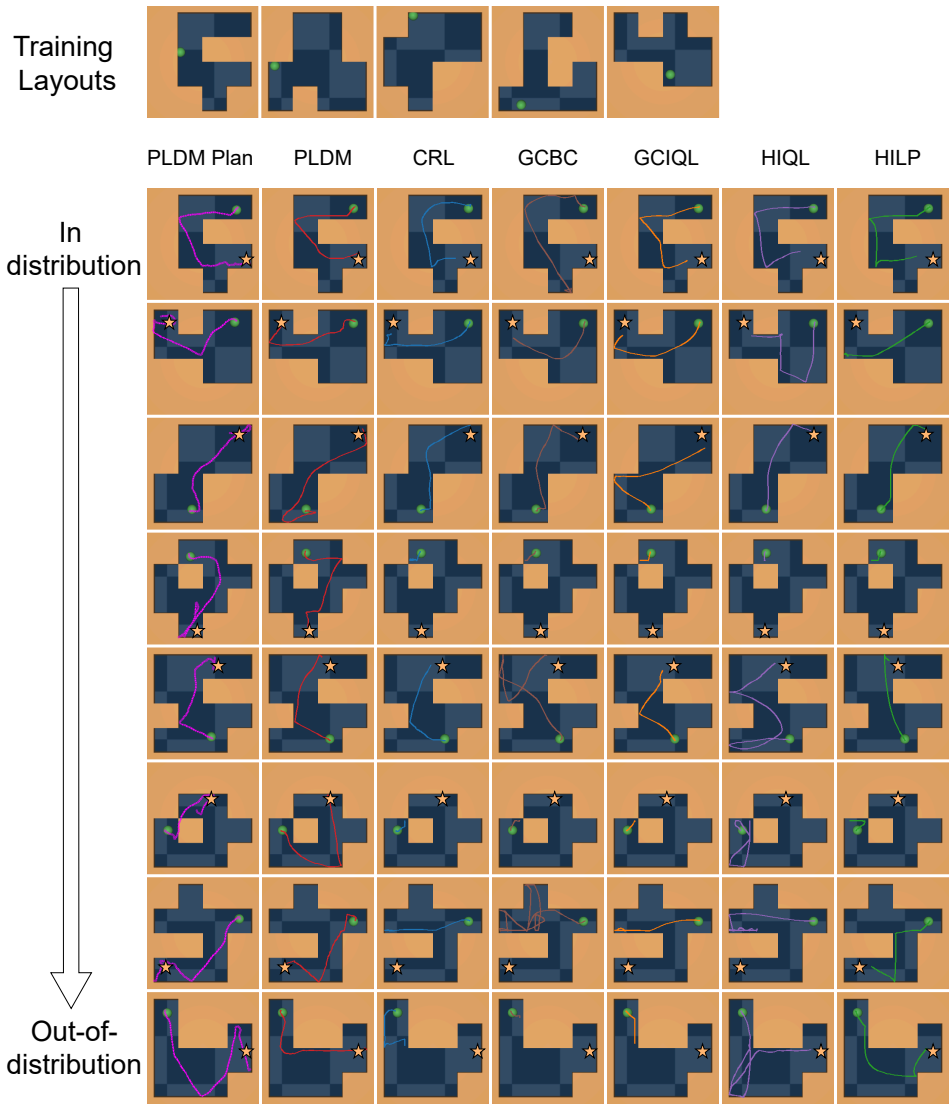

Figure 8: **Top**: The training layouts used in the 5 layout setting. **Middle**: Trajectories of different agents navigating an unseen maze layout towards goal at test time. As the layouts become increasingly out-of-distribution, only PLDN consistently succeeds. Layouts can be represented as a 4x4 array, with each value being either a wall or empty space. The distribution shift is quantified by the minimum edit distance between a given test layout and the closest training layout. The top row corresponds to an in-distribution layout with a minimum edit distance of 0, and with each subsequent row, the minimum edit distance increases by 1 incrementally.

C Environments and Datasets

C.1 Two-Rooms Environment

We build our own top-down navigation environment. It is implemented in PyTorch [54], and supports GPU acceleration. The environment does not model momentum, i.e. the agent does not have velocity, and is moved by the specified action vector at each step. When the action takes the agent through a wall, the agent is moved to the intersection point between the action vector and the wall. We generate the specified datasets and save them to disk for our experiments. The datasets generation takes under 30 minutes.

C.2 Diverse PointMaze

Here, we build upon the Mujoco PointMaze environment [66], which contains a point mass agent with a 4D state vector $(\text{global } x, \text{global } y, v_x, v_y)$, where v is the agent velocity. To allow our models to perceive the different maze layouts, we use as model input a top down view of the maze rendered as $(64, 64, 3)$ RGB image tensor instead of relying on $(\text{global } x, \text{global } y)$ directly.

Mujoco PointMaze allows for customization of the maze layout via a grid structure, where a grid cell can either be a wall or space. We opt for a 4×4 grid (excluding outer wall). Maze layouts are generated randomly. Only the following constraints are enforced: 1) all the space cells are interconnected, 2) percentage of space cells range from 50% to 75%.

We set action repeat to 4 for our version of the environment.

C.2.1 Dataset Generation

We produce four training datasets with the following parameters:

# Transitions	# layouts	# episodes per layout	episode length
1000000	5	2000	100
1000000	10	1000	100
1000000	20	500	100
1000000	40	250	100

Table 3: Details for Diverse PointMaze datasets

Each episode is collected by setting the $(\text{global } x, \text{global } y)$ at a random location in the maze, and agent velocity (v_x, v_y) by randomly sampling a 2D vector with $\|v\| \leq 5$, given that v_x and v_y are clipped within range of $[-5, 5]$ in the environment.

C.2.2 Evaluation

All the test layouts during evaluation are disjoint from the training layouts. For each layout, trials are created by randomly sampling a start and goal position guaranteed to be at least 3 cells away on the maze. The same set of layouts and trials are used to evaluate all agents for a given experimental setting.

We evaluate agents in two scenarios: 1) How agents perform on test layouts when trained on various number of train layouts; 2) Given a constant number of training layouts, how agents perform on test maps with varying degrees of distribution shift from the training layouts.

For scenario 1), we evaluate the agents on 40 randomly generated test layouts, 1 trial per layout.

For scenario 2), we randomly generate test layouts and partition them into groups of 5, where all the layouts in each group have the same degree of distribution shift from train layout as defined by metric D_{min} defined as the following:

Given train layouts $\{L^1_{\text{train}}, L^2_{\text{train}}, ...L^N_{\text{train}}\}$, test layout L_{test}, and let $d(L_1, L_2)$ represents the edit distance between two layouts L_1 and L_2's binary grid representation. We quantify the distribution shift of L_{test} as $D_{\min} = \min_{i \in \{1,2,...,N\}} d(L_{\text{test}}, L^{(i)}_{\text{train}})$.

In this second scenario we evaluate 5 trials per layout, thus a total of $5 \times 5 = 25$ per group.

C.2.3 Results for Single Maze Setting

Table 4: Results averaged over 3 seeds ± std

Method	Success rate
PLDM	0.990 ± 0.001
CRL	0.980 ± 0.001
GCBC	0.970 ± 0.024
GCIQL	1.000 ± 0.000
HIQL	1.000 ± 0.000
HILP	1.000 ± 0.000

C.3 Ant U-Maze

To investigate whether our findings generalize to environments with more complicated control dynamics, we test the methods on the Ant U-Maze environment [66] with 8-dimensional action space and 29-dimensional state space. Similar to our previous analysis on Two-Rooms, we showcase the trajectory stitching capabilities of different methods.

C.3.1 Dataset Generation

To collect the dataset, we use a pretrained expert directional policy from Park et al. [51] to generate 5M transitions of exploratory data, where we resample a new direction every 10 steps, and apply Gaussian noise with a standard deviation of 1.0 to every action.

C.3.2 Evaluation

For evaluation, the quadruped is randomly initialized at either the left bottom or right bottom corner, while the goal location is at the opposite diagonal corner, thus requiring the ant to make 1 turn. Each method is evaluated on 10 trials.

D Models

For CRL, GCBC, GCIQL, and HIQL we use the implementations from the repository[1] of OGBench [51]. Likewise, for HILP we use the official implementation[2] from its authors.

For the Diverse PointMaze environment, to keep things consistent with our implementation of PLDM (D.1.4), instead of using frame stacking, we append the agent velocity directly to the encoder output.

D.1 PLDM

D.1.1 Objective for collapse prevention

To prevent collapse, we introduce a VICReg-based [4] objective. We modify it to apply variance objective across the time dimension to encourage features to capture information that changes, as

[1] https://github.com/seohongpark/ogbench
[2] https://github.com/seohongpark/HILP

opposed to information that stays fixed [61]. The objective to prevent collapse is defined as follows:

$$\mathcal{L}_{\text{var}} = \frac{1}{HD}\sum_{t=0}^{H}\sum_{j=0}^{D}\max(0, \gamma - \sqrt{\text{Var}(Z_{t,:,j}) + \epsilon})$$

$$C(Z_t) = \frac{1}{N-1}(Z_t - \bar{Z}_t)^\top (Z_t - \bar{Z}_t),\ \bar{Z} = \frac{1}{N}\sum_{b=1}^{N} Z_{t,b}$$

$$\mathcal{L}_{\text{cov}} = \frac{1}{H}\sum_{t=0}^{H}\frac{1}{D}\sum_{i\neq j}[C(Z_t)]_{i,j}^2$$

$$\mathcal{L}_{\text{IDM}} = \sum_{t=0}^{H}\frac{1}{N}\sum_{b=0}^{N}\|a_{t,b} - \text{MLP}(Z_{(t,b)}, Z_{(t+1,b)})\|_2^2$$

We also apply a tunable objective to enforce the temporal smoothness of learned representations:

$$\mathcal{L}_{\text{time-sim}} = \sum_{t=0}^{H-1}\frac{1}{N}\sum_{b=0}^{N}\|Z_{t,b} - Z_{t+1,b}\|_2^2$$

The combined objective is a weighted sum of above:

$$\mathcal{L}_{\text{JEPA}} = \mathcal{L}_{\text{sim}} + \alpha\mathcal{L}_{\text{var}} + \beta\mathcal{L}_{\text{cov}} + \delta\mathcal{L}_{\text{time-sim}} + \omega\mathcal{L}_{\text{IDM}}$$

D.1.2 Ablations of Objective Components

We conduct a careful ablation study over each loss component by setting its coefficient to zero. Two-Room ablations are performed in the optimal setting with sequence length 90, dataset size 3M, and all expert data. Diverse Maze ablations are performed in the 5 training maps setting.

Ablation	Success rate (Two-Rooms)	Success rate (Diverse Maze)
–	98.0 ± 1.5	98.7 ± 2.8
var coeff (α)	13.4 ± 9.2	11.4 ± 6.5
cov coeff (β)	29.2 ± 4.4	7.8 ± 4.1
time sim coeff (δ)	71.0 ± 3.0	95.6 ± 3.2
IDM coeff (ω)	98.0 ± 1.5	75.5 ± 8.2

D.1.3 Model Details for Two-Rooms

We use the same Impala Small Encoder used by the other methods from OGBench [51]. For predictor, we use the a 2-layer Gated recurrent unit [14] with 512 hidden dimensions; the predictor input at timestep t is a 2D displacement vector representing agent action at timestep t; while the initial hidden state is $h_\theta(s_0)$, or the encoded state at timestep 0. A single layer normalization layer is applied to the encoder and predictor outputs across all timesteps. Parameter counts are the following:

```
total params: 2218672
encoder params: 1426096
predictor params: 793600
```

D.1.4 Model Details for Diverse PointMaze Environment

For the Diverse PointMaze environment, we use convolutional networks for both the encoder and predictor. To fully capture the agent's state at timestep t, we first encode the top down view of the maze to get a spatial representation of the environment $h_\theta : \mathbb{R}^{3\times64\times64} \to \mathbb{R}^{16\times26\times26}, z^{env} = h_\theta(s^{env})$. We incorporate the agent velocity by first transforming it into planes $\text{Expander2D} : \mathbb{R}^2 \to \mathbb{R}^{2\times26\times26}, s^{vp} = \text{Expander2D}(s^v)$, where each slice $s^{vp}[i]$ is filled with $s^v[i]$. Then, we concatenate the expanded velocity tensor with spatial representation along the channel dimension to get our overall representation: $z = \text{concat}(s^{vp}, z^{env}, \text{dim} = 0) \in \mathbb{R}^{18\times26\times26}$.

For the predictor input, we concatenate the state $s_t \in \mathbb{R}^{18\times26\times26}$ with the expanded action $\text{Expander2D}(a_t) \in \mathbb{R}^{2\times26\times26}$ along the channel dimension. The predictor output has the same dimension as the representation: $\hat{z} \in \mathbb{R}^{18\times26\times26}$. Both the encodings and predictions are flattened for computing the VicReg and IDM objectives.

We set the planning-frequency (Section 3.3) in MPPI to $k = 4$ for this environment.

The full model architecture is summarized using PyTorch-like notations.

```
total params: 53666
encoder params: 33296
predictor params: 20370

PLDM(
    (backbone): MeNet6(
        (layers): Sequential(
            (0): Conv2d(3, 16, kernel_size=(5, 5), stride=(1, 1))
            (1): GroupNorm(4, 16, eps=1e-05, affine=True)
            (2): ReLU()
            (3): Conv2d(16, 32, kernel_size=(5, 5), stride=(2, 2))
            (4): GroupNorm(8, 32, eps=1e-05, affine=True)
            (5): ReLU()
            (6): Conv2d(32, 32, kernel_size=(3, 3), stride=(1, 1))
            (7): GroupNorm(8, 32, eps=1e-05, affine=True)
            (8): ReLU()
            (9): Conv2d(32, 32, kernel_size=(3, 3), stride=(1, 1), padding=(1, 1))
            (10): GroupNorm(8, 32, eps=1e-05, affine=True)
            (11): ReLU()
            (12): Conv2d(32, 16, kernel_size=(1, 1), stride=(1, 1))
        )
        (propio_encoder): Expander2D()
    )
    (predictor): ConvPredictor(
        (layers): Sequential(
            (0): Conv2d(20, 32, kernel_size=(3, 3), stride=(1, 1), padding=(1, 1))
            (1): GroupNorm(4, 32, eps=1e-05, affine=True)
            (2): ReLU()
            (3): Conv2d(32, 32, kernel_size=(3, 3), stride=(1, 1), padding=(1, 1))
            (4): GroupNorm(4, 32, eps=1e-05, affine=True)
            (5): ReLU()
            (6): Conv2d(32, 18, kernel_size=(3, 3), stride=(1, 1), padding=(1, 1))
        )
        (action_encoder): Expander2D()
    )
)
```

D.1.5 Model Details for Ant-U-Maze

We encode the global (x, y) position using a 2-layer MLP into a 256 dimensional embedding, and concatenate it with the rest of the raw proprioceptive state to make our overall state representation. Our predictor is a 3-layer MLP with ensemble size of 5. During training, variance and covariance regularization is only applied on the part of the representation for (x, y) (first 256 dimensions), since the rest of the proprioceptive state are not encoded and therefore do not collapse.

```
total params: 1080615
encoder params: 9120
predictor params: 1072007

PLDM(
    (backbone): MLPEncoder(
        (globa_xy_encoder): Sequential(
            (0): Linear(in_features=2, out_features=32, bias=True)
            (1): LayerNorm((32,), eps=1e-05, elementwise_affine=True)
            (2): Mish(inplace=True)
            (3): Linear(in_features=32, out_features=256, bias=True)
```

```
            (4): LayerNorm((256,), eps=1e-05, elementwise_affine=True)
        )
        (proprio_encoder): Identity()
    )
    (predictor): MLPPredictor(
        (layers): Sequential(
            (0): Linear(in_features=291, out_features=256, bias=True)
            (1): LayerNorm((256,), eps=1e-05, elementwise_affine=True)
            (2): Mish(inplace=True)
            (3): Linear(in_features=256, out_features=256, bias=True)
            (4): LayerNorm((256,), eps=1e-05, elementwise_affine=True)
            (5): Mish(inplace=True)
            (6): Linear(in_features=256, out_features=283, bias=True)
            (7): LayerNorm((283,), eps=1e-05, elementwise_affine=True)
        )
    )
)
```

E Effects of Uncertainty Regularization via Ensembles

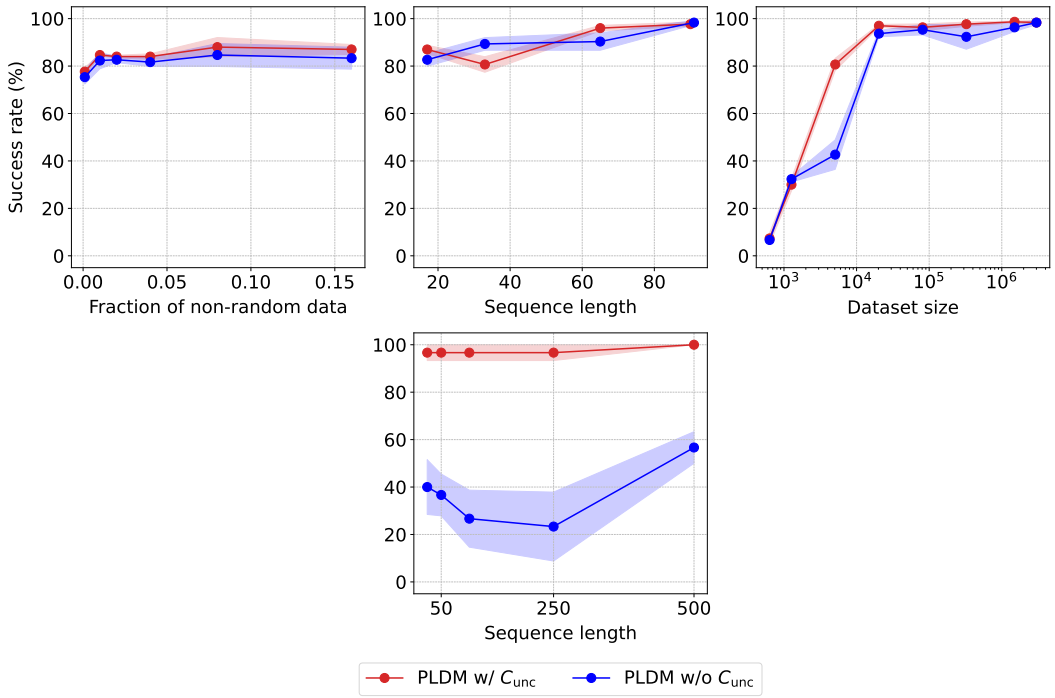

Figure 9: **Top Row**: Two-Rooms environment. **Bottom Row**: AntMaze environment.

F Analyzing planning time of PLDM

In order to estimate how computationally expensive it is to run planning with a latent dynamics model, we evaluate PLDM, GCIQL, and HIQL on 25 episodes in the Two-Rooms environment. Each episode consists of 200 steps. We record the average time per episode and the standard deviation. We omit HILP, GCBC, or CRL because the resulting policy architecture is the same, making the evaluation time identical to that of GCIQL. HIQL takes more time due to the hierarchy of policies. When replanning every step, PLDM is slower than the policies. However, PLDM can match the latencies of policies by replanning less frequently with negligible performance drop.

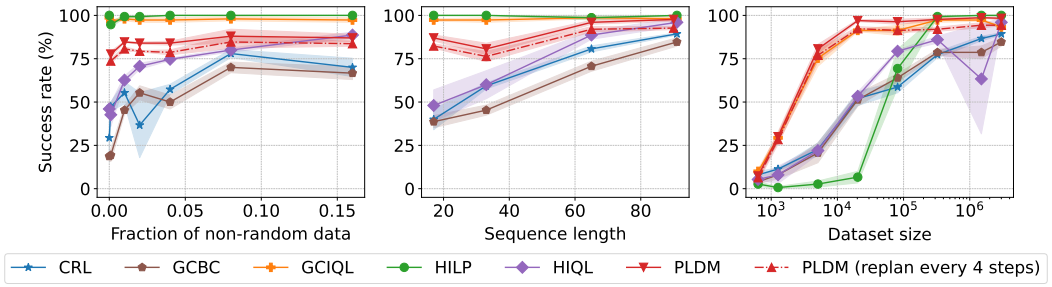

Figure 10: **Comparing PLDM's performance under fixed inference time compute budget on two-rooms.** We see that across two-rooms experiments, PLDM performs only slightly worse when replanning every 4 steps compared to replanning every step.

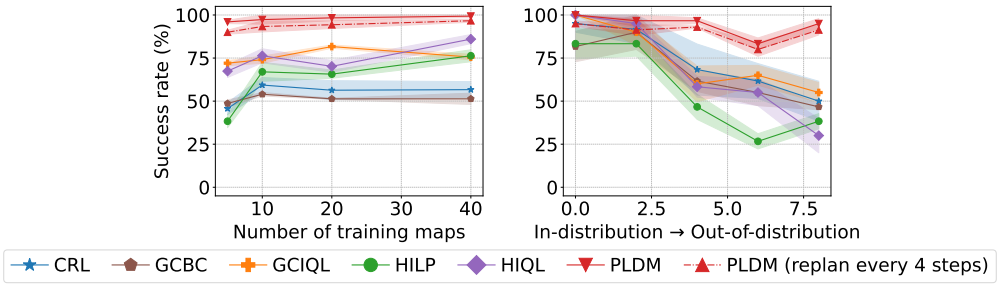

Figure 11: **Evaluating PLDM's performance under fixed inference time compute budget on diverse maze.** Similarly to two-rooms, we only see a minor degradation in performnace

Table 5: Time of evaluation on one episode in Two-Rooms environment. Time is averaged across 25 episodes. PLDM success rates are normalized against the setting that replans every step. PLDM can match the latencies of GCIQL and HIQL by replanning less frequently with neligible cost to performance.

Method	Replan Every	Time per episode (seconds)	Normalized Success Rate
PLDM	1	16.0 ± 0.13	1.00
PLDM	4	4.8 ± 0.09	0.95
PLDM	16	2.6 ± 0.07	0.90
PLDM	32	2.2 ± 0.07	0.62
GCIQL	–	3.6 ± 0.10	–
HIQL	–	4.0 ± 0.08	–

F.1 Evaluating PLDM Performance With Adjusted Inference Compute Budget

As we see in Table 5, replanning every 4 steps brings PLDM close to other methods' inference speed. In order to further compare how PLDM compares to other methods when inference time compute is fixed between methods, we run additional evaluations, and report them in Figure 10 and Figure 11.

G Extended Baselines: Input Reconstruction Learning and TD-MPC2

In this section, we evaluate reconstruction-based objectives for training the encoder and dynamics model, as well as TD-MPC2 [28]. For reconstruction, we compare two approaches: one based on Dreamer [25], and one that replaces our VICReg objective with pixel reconstruction.

Dreamer We adapt DreamerV3 [26] to our setting by:

- Removing rewards during training and using only the reconstruction loss;
- Omitting policy learning, instead planning via latent representation distance, just like we did for PLDM. Since the representations DreamerV3 uses are discrete, we use KL divergence instead of L2 distance. We note that this is not what DreamerV3 architecture was designed

Table 6: **Comparing reconstruction-based latent-dynamics learning and TDMPC-2 to other baselines.** We test the methods on good-quality data in the two-rooms environment. We see that reconstruction-based methods perform significantly worse than PLDM and other baselines. TD-MPC2 fails to learn altogether due to collapse, and performs poorly even with the added IDM objective.

Method	Success rate
CRL	89.3 ± 1.2
GCBC	86.0 ± 4.5
GCIQL	98.0 ± 0.9
HILP	100.0 ± 0.0
HIQL	96.4 ± 3.0
PLDM	97.4 ± 1.3
DreamerV3	24.0 ± 6.9
Reconstruction	26.2 ± 13.9
TD-MPC2	0.0 ± 0.0
TD-MPC2 + IDM	35.0 ± 0.0

for, making this comparison flawed. However, we believe it serves to highlight that compared to DreamerV3, PLDM is designed for a very different setting in terms of available data.

Reconstruction As opposed to Dreamer, this baseline uses the same architecture of the encoder and dynamics as PLDM instead of RSSM, and only replaces the VICReg objective with a reconstruction term. The architecture of the decoder mirrors that of the encoder.

TD-MPC2 Like Dreamer models, TD-MPC2 [28] also relies on rewards to learn its representions. In order to adapt TD-MPC2 to our setting, we remove the reward prediction component, and only keep the objective enforcing consistency between the predictor and encoder outputs.

Results are shown in Table 6. We test all methods on the two-rooms environment described in Section 4.1. We use good-quality data, with long trajectories and good transition coverage. We find that pixel observation reconstruction is not a good objective to learn representations, and using it results in poor planning performance. TD-MPC2 collapses altogether, achieving 0% success rate. To prevent collpase, we add inverse dynamics modelling (IDM), which somewhat improves performnace, although it is still far behind other methods. We only tested one seed for TD-MPC2 + IDM.

H Analyzing Statistical Significance of Results

In order to analyze whether the results in this paper are statistically significant, we perform Welch's t-test to compare the performance of PLDM to other methods. Because 5 seeds is not enough for statistical tests, we pool results across settings and show results in Table 7. We also run additional seeds for certain selected settings to get a total of 10 seeds per method, and show results of statistical analysis in Table 8. Overall, we see that the results are significant, except for certain settings comparing to HILP and GCIQL, which aligns with our findings.

Table 7: Statistical significance of results (pooled). ✓ means that Welch's t-test showed that PLDM is better than the corresponding method when pooling results across seeds and dataset parameters.

	Sequence length	Fraction of non-random data	Dataset size	Number of training maps	In-distribution → Out-of-distribution
CRL	✓(p=1.68e-03)	✓(p=8.46e-07)	✓(p=1.13e-02)	✓(p=3.43e-10)	✓(p=4.02e-03)
GCBC	✓(p=4.25e-04)	✓(p=1.46e-08)	✓(p=7.26e-03)	✓(p=3.71e-20)	✓(p=1.94e-05)
GCIQL	✗	✗	✗	✓(p=1.29e-12)	✓(p=1.22e-03)
HILP	✗	✗	✓(p=2.11e-02)	✓(p=6.54e-06)	✓(p=4.10e-05)
HIQL	✓(p=2.21e-02)	✓(p=9.26e-05)	✓(p=2.39e-02)	✓(p=2.84e-06)	✓(p=9.01e-03)

Table 8: Statistical significance of results for selected datasets. ✓ means that Welch's t-test showed that PLDM is better than the corresponding method results across 10 seeds.

	Sequence length 17	Fraction of non-random data 0%	Dataset size 20312
CRL	✓(p=3.82e-11)	✓(p=1.13e-07)	✓(p=6.76e-11)
GCBC	✓(p=1.54e-12)	✓(p=5.75e-10)	✓(p=1.88e-14)
GCIQL	✗	✗	✗
HILP	✗	✗	✓(p=2.49e-19)
HIQL	✓(p=8.89e-05)	✓(p=2.83e-07)	✓(p=2.65e-11)

I Analyzing HILP's Out-of-Distribution Generalization

To understand HILP's poor generalization to out-of-distribution (OOD) maze layouts, we visualize the distance in HILP's learned latent representation space. HILP learns a latent representation $\phi(s)$, such that $\|\phi(s) - \phi(s_g)\|_2$ is equal to the lowest number of transitions needed to traverse from s to s_g. We hypothesize that ϕ fails to generalize to out-of-distribution maze layouts, resulting in incorrect predicted distances and in the failure of the goal-conditioned policy. We visualize the distances on in-distribution and out-of-distribution layouts for an encoder ϕ trained on 5 different layouts in Appendix I. We see that HILP distances are meaningful only on in-distribution layouts, and are very noisy on out-of-distribution layouts. This failure of the latent-space distance to generalize to out-of-distribution layouts confirms our hypothesis, and highlights the strength of PLDM.

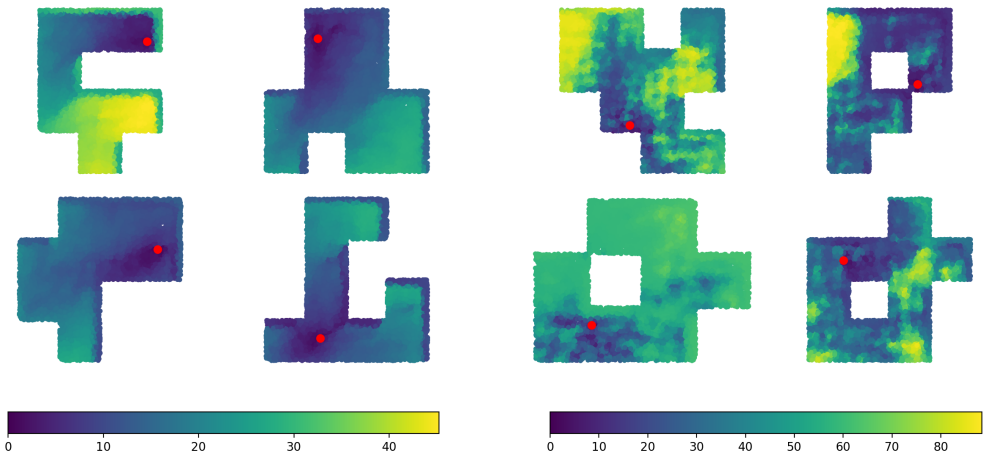

(a) HILP distances on in-distribution maze layouts (b) HILP distances on out-of-distribution maze layouts

Figure 12: HILP learns representations of states such that distance in representation space between a pair of states is equal to the number of steps needed to go between steps. These plots visualize the distance from the state denoted with a red dot to other states across the maze. (a) We see that on an in-distribution maze, the distances increase smoothly and mostly reflect the number of steps needed to go between states. (b) We see that on an out-of distribution maze, the representation space distances no longer make sense.

J Hyperparameters

J.1 CRL, GCBC, GCIQL, HIQL, HILP

Unless listed below, all hyperparameters remain consistent with default values from OGBench[1] and HILP[2] repositories

J.1.1 Two-Rooms

To tune hyperparameters, we ran 1 grid search for good quality data, then another grid search for sequence length 17, then tested both on all settings. In grid searches, we searched over learning rate, expectiles (for GCIQL, HILP, and HIQL), and the probability of sampling random goal. For CRL and GCBC, we ended up using default OGBench parameters. The other parameters are described below:

HILP. We used learning rate of 3e-4, expectile of 0.7, and skill expectile of 0.7 in all settings.

GCIQL. For settings with dataset size of 634 as well as for good quality data, we used expectile 0.7, learning rate 3e-4, BC coefficient of 0.3, and 0 probability of sampling random goal. For all other settings, we used learning rate 3e-4, expectile of 0.7, BC coefficient of 0.003, and probability of sampling a random goal 0.3.

HIQL. For sequence length 17 and 33, we used learning rate of 3e-5, expectile of 0.7, AWR temperature of 3.0 (both high and low levels), and probability of sampling a random goal of 0.6. For all other settings, we used learning rate of 3e-4, expectile of 0.7, AWR temperature of 3.0 (both high and low levels), and probability of sampling a random goal of 0.

J.1.2 Diverse PointMaze

Table 9: Dataset-specific hyperparameters of CRL, GCBC, and HILP for the Diverse PointMaze environment. For HILP, we set the same value for expectile and skill expectile.

Dataset	CRL	GCBC	HILP	
	LR	LR	LR	Expectile
5 layouts	0.0003	0.0003	0.0001	0.9
10 layouts	0.0003	0.0001	0.0001	0.9
20 layouts	0.0003	0.0001	0.0001	0.9
40 layouts	0.0003	0.0001	0.0001	0.9

Table 10: Dataset-specific hyperparameters of GCIQL and HIQL for the Diverse PointMaze environment.

Dataset	GCIQL				HIQL			
	LR	Expectile	BC Coeff.	Prob Rand Goal	LR	Expectile	AWR Temp.	Prob Rand Goal
5 layouts	0.0003	0.6	0.3	0.15	0.00003	0.6	1.0	0.6
10 layouts	0.0003	0.6	0.3	0.15	0.0001	0.7	3.0	0.0
20 layouts	0.0003	0.6	0.3	0.15	0.00003	0.6	1.0	0.6
40 layouts	0.0003	0.6	0.3	0.15	0.0001	0.7	3.0	0.0

J.1.3 Ant U-Maze

Table 11: Ant-Umaze: dataset-specific hyperparameters for CRL, GCBC, and HILP, parsed from run names.

Seq Len	CRL			GCBC	HILP	
	LR	BC Coeff.	Prob Rand Goal	LR	LR	Expectile (skill / actor)
25	3e-5	0.1	0.3	3e-3	3e-4	0.6 / 0.8
50	3e-5	0.1	0.3	3e-3	3e-4	0.6 / 0.8
100	3e-4	0.1	0.0	3e-3	3e-4	0.6 / 0.8
250	3e-4	0.1	0.0	3e-3	3e-4	0.6 / 0.8
500	3e-4	0.1	0.0	3e-3	3e-4	0.6 / 0.8

Table 12: Ant-Umaze: dataset-specific hyperparameters for GCIQL and HIQL parsed from run names.

Seq Len	GCIQL				HIQL			
	LR	Expectile	BC Coeff.	Prob Rand Goal	LR	Expectile	AWR Temp.	Prob Rand Goal
25	3e-5	0.9	0.15	0.15	3e-4	0.6	3.0	0.6
50	3e-5	0.9	0.15	0.15	3e-4	0.6	3.0	0.6
100	3e-5	0.9	0.15	0.15	3e-4	0.6	3.0	0.6
250	3e-4	0.9	0.3	0.0	3e-4	0.6	3.0	0.6
500	3e-4	0.9	0.3	0.0	3e-4	0.6	3.0	0.6

J.2 PLDM

J.2.1 Two-Rooms

The best case setting is sequence length = 91, dataset size = 3M, non-random % = 100, wall crossing % $\approx$ 35. For our experiments we vary each of the above parameters individually.

Table 13: Dataset-agnostic hyperparameters for Two-Rooms

Hyperparameter	**Value**
Batch Size	64
Predictor Horizon (H)	16
Optimizer	Adam
Scheduler	Cosine
Ensemble size K	5
ω	0
MPPI noise σ	5
MPPI # samples	500
MPPI λ	0.005
Planner $C_{\text{uncertainty}}$ coeff β	0.0001
Planner $C_{\text{uncertainty}}$ coeff γ	0.9

For the dataset specific hyperparameters, we tune the following parameters from Appendix D.1.1:

Table 14: Dataset specific hyperparameters for Two-Rooms

Dataset	**LR**	α	β	δ
Sequence length = 91	0.0007	4.0	6.9	0.75
Sequence length = 65	0.0003	5.0	6.9	0.75
Sequence length = 33	0.0014	3.5	6.9	0.75
Sequence length = 17	0.0028	3.0	6.9	0.75
Dataset size = 634	0.0030	2.2	13.0	0.50
Dataset size = 1269	0.0010	2.2	13.0	0.50
Dataset size = 5078	0.0005	2.2	13.0	0.90
Dataset size = 20312	0.0030	2.2	13.0	0.50
Dataset size = 81250	0.0010	2.2	13.0	0.50
Dataset size = 325k	0.0010	4.0	6.9	0.75
Dataset size = 1500k	0.0010	4.0	6.9	0.75
Non-random % = 0.001	0.0007	3.9	6.9	0.74
Non-random % = 0.01	0.0007	3.9	6.5	0.19
Non-random % = 0.02	0.0007	3.9	6.5	0.72
Non-random % = 0.04	0.0007	3.9	6.5	0.65
Non-random % = 0.08	0.0007	3.9	6.5	0.24
Non-random % = 0.08	0.0007	3.9	6.5	0.24
Wall crossing % = 0	0.0007	4.0	6.9	0.75

J.2.2 Diverse PointMaze

Table 15: Dataset-agnostic hyperparameters for Diverse PointMaze

Hyperparameter	Value
Epochs	5
Batch Size	128
Predictor Horizon (H)	16
Optimizer	Adam
Scheduler	Cosine
Ensemble size K	1
MPPI noise σ	5
MPPI # samples	500
MPPI λ	0.0025

Table 16: Dataset specific hyperparameters for Diverse PointMaze

Dataset	LR	α	β	δ	ω
# map layouts = 5	0.04	35.0	12.0	0.1	5.4
# map layouts = 5	0.04	35.0	12.0	0.1	5.4
# map layouts = 20	0.05	54.5	15.5	0.1	5.2
# map layouts = 40	0.05	54.5	15.5	0.1	5.2

J.2.3 Ant-U-Maze

Table 17: Dataset-agnostic hyperparameters for Ant-U-Maze

Hyperparameter	Value
Epochs	5
Batch Size	64
Predictor Horizon (H)	16
Optimizer	Adam
Scheduler	Cosine
Ensemble size K	5
α	26.2
β	0.5
δ	8.1
ω	0.58
MPPI noise σ	5
MPPI # samples	500
MPPI λ	0.0025
Planner $C_{\text{uncertainty}}$ coeff β	1
Planner $C_{\text{uncertainty}}$ coeff γ	0.9

Table 18: Dataset-specific hyperparameters for Ant-U-Maze

Dataset	LR
Sequence length = 25	0.006
Sequence length = 50	0.004
Sequence length = 100	0.003
Sequence length = 250	0.001
Sequence length = 500	0.001

J.3 Further related work

Offline RL. This field aims to learn behaviors purely from offline data without online interactions. As opposed to imitation learning [80], offline RL is capable of learning policies that are better than the policy collecting the data. However, a big challenge is preventing the policy from selecting actions that were not seen in the dataset. CQL [36] relies on model conservatism to prevent the learned policy from being overly optimistic about trajectories not observed in the data. IQL [33] introduces an objective that avoids evaluating the Q-function on state-action pairs not seen in the data to prevent value overestimation. MOPO [78] is a model-based approach to learning from offline data, and uses model disagreement to constrain the policy. See [41] for a more in-depth survey.

Foundation models in RL. Recently, following the success of NLP, the RL community put a lot of effort into training large sequence models, which sparked dataset collection efforts like Open-X-Embodiment [15] and DROID [31]. Large datasets have enabled training models such as RT-2 [10] and Octo [48]. See [75] for a more extensive survey on the topic.

Training representations for RL. Another way to use large amounts of data to improve RL agents is using self-supervised learning (SSL). CURL [38] introduce an SSL objective in addition to the standard RL objectives. Later works also explore using a separate pre-training stage [47, 58, 82]. Zhou et al. [83] show that pre-trained visual representations from DINO [13, 50] can be used to learn a word model for planning.

K Discussion of Computational Costs

All experiments require only a single GPU, and take up to 1 day when using an Nvidia V100 GPU. We estimate the total computational cost of the experiments included in the paper and in the research process to be between 500 and 2000 GPU days.

L Limitations

All our experiments were conducted in navigation environments, excluding robot manipulation or partially observable settings. However, we argue that the conceptual understanding of the effects of data quality on the investigated methods will hold, as even in the relatively simple setting, we see many recent methods break down in surprising ways. Another limitation lies in the fact that PLDM is about 4 times slower during inference, although in Appendix F we find that even when limited to the same budget of inference compute as model-free methods, PLDM retains most of its performnace.

NeurIPS Paper Checklist

The checklist is designed to encourage best practices for responsible machine learning research, addressing issues of reproducibility, transparency, research ethics, and societal impact. Do not remove the checklist: **The papers not including the checklist will be desk rejected.** The checklist should follow the references and follow the (optional) supplemental material. The checklist does NOT count towards the page limit.

Please read the checklist guidelines carefully for information on how to answer these questions. For each question in the checklist:

- You should answer [Yes] , [No] , or [NA] .
- [NA] means either that the question is Not Applicable for that particular paper or the relevant information is Not Available.
- Please provide a short (1–2 sentence) justification right after your answer (even for NA).

The checklist answers are an integral part of your paper submission. They are visible to the reviewers, area chairs, senior area chairs, and ethics reviewers. You will be asked to also include it (after eventual revisions) with the final version of your paper, and its final version will be published with the paper.

The reviewers of your paper will be asked to use the checklist as one of the factors in their evaluation. While "[Yes] " is generally preferable to "[No] ", it is perfectly acceptable to answer "[No] " provided a proper justification is given (e.g., "error bars are not reported because it would be too computationally expensive" or "we were unable to find the license for the dataset we used"). In general, answering "[No] " or "[NA] " is not grounds for rejection. While the questions are phrased in a binary way, we acknowledge that the true answer is often more nuanced, so please just use your best judgment and write a justification to elaborate. All supporting evidence can appear either in the main paper or the supplemental material, provided in appendix. If you answer [Yes] to a question, in the justification please point to the section(s) where related material for the question can be found.

IMPORTANT, please:

- **Delete this instruction block, but keep the section heading "NeurIPS Paper Checklist"**,
- **Keep the checklist subsection headings, questions/answers and guidelines below.**
- **Do not modify the questions and only use the provided macros for your answers**.

1. **Claims**

   Question: Do the main claims made in the abstract and introduction accurately reflect the paper's contributions and scope?

   Answer: [Yes]

   Justification: Main claims are supported by our experiments.

   Guidelines:

   - The answer NA means that the abstract and introduction do not include the claims made in the paper.
   - The abstract and/or introduction should clearly state the claims made, including the contributions made in the paper and important assumptions and limitations. A No or NA answer to this question will not be perceived well by the reviewers.
   - The claims made should match theoretical and experimental results, and reflect how much the results can be expected to generalize to other settings.
   - It is fine to include aspirational goals as motivation as long as it is clear that these goals are not attained by the paper.

2. **Limitations**

   Question: Does the paper discuss the limitations of the work performed by the authors?

   Answer: [Yes]

   Justification: We have a limitations section in the conclusion.

Guidelines:

- The answer NA means that the paper has no limitation while the answer No means that the paper has limitations, but those are not discussed in the paper.
- The authors are encouraged to create a separate "Limitations" section in their paper.
- The paper should point out any strong assumptions and how robust the results are to violations of these assumptions (e.g., independence assumptions, noiseless settings, model well-specification, asymptotic approximations only holding locally). The authors should reflect on how these assumptions might be violated in practice and what the implications would be.
- The authors should reflect on the scope of the claims made, e.g., if the approach was only tested on a few datasets or with a few runs. In general, empirical results often depend on implicit assumptions, which should be articulated.
- The authors should reflect on the factors that influence the performance of the approach. For example, a facial recognition algorithm may perform poorly when image resolution is low or images are taken in low lighting. Or a speech-to-text system might not be used reliably to provide closed captions for online lectures because it fails to handle technical jargon.
- The authors should discuss the computational efficiency of the proposed algorithms and how they scale with dataset size.
- If applicable, the authors should discuss possible limitations of their approach to address problems of privacy and fairness.
- While the authors might fear that complete honesty about limitations might be used by reviewers as grounds for rejection, a worse outcome might be that reviewers discover limitations that aren't acknowledged in the paper. The authors should use their best judgment and recognize that individual actions in favor of transparency play an important role in developing norms that preserve the integrity of the community. Reviewers will be specifically instructed to not penalize honesty concerning limitations.

3. **Theory assumptions and proofs**

   Question: For each theoretical result, does the paper provide the full set of assumptions and a complete (and correct) proof?

   Answer: [NA]

   Justification: This paper is empirical in nature, no theoretical results were provided.

   Guidelines:

   - The answer NA means that the paper does not include theoretical results.
   - All the theorems, formulas, and proofs in the paper should be numbered and cross-referenced.
   - All assumptions should be clearly stated or referenced in the statement of any theorems.
   - The proofs can either appear in the main paper or the supplemental material, but if they appear in the supplemental material, the authors are encouraged to provide a short proof sketch to provide intuition.
   - Inversely, any informal proof provided in the core of the paper should be complemented by formal proofs provided in appendix or supplemental material.
   - Theorems and Lemmas that the proof relies upon should be properly referenced.

4. **Experimental result reproducibility**

   Question: Does the paper fully disclose all the information needed to reproduce the main experimental results of the paper to the extent that it affects the main claims and/or conclusions of the paper (regardless of whether the code and data are provided or not)?

   Answer: [Yes]

   Justification: We provide hyperparameters and code to reproduce results.

   Guidelines:

   - The answer NA means that the paper does not include experiments.

- If the paper includes experiments, a No answer to this question will not be perceived well by the reviewers: Making the paper reproducible is important, regardless of whether the code and data are provided or not.
- If the contribution is a dataset and/or model, the authors should describe the steps taken to make their results reproducible or verifiable.
- Depending on the contribution, reproducibility can be accomplished in various ways. For example, if the contribution is a novel architecture, describing the architecture fully might suffice, or if the contribution is a specific model and empirical evaluation, it may be necessary to either make it possible for others to replicate the model with the same dataset, or provide access to the model. In general. releasing code and data is often one good way to accomplish this, but reproducibility can also be provided via detailed instructions for how to replicate the results, access to a hosted model (e.g., in the case of a large language model), releasing of a model checkpoint, or other means that are appropriate to the research performed.
- While NeurIPS does not require releasing code, the conference does require all submissions to provide some reasonable avenue for reproducibility, which may depend on the nature of the contribution. For example
  (a) If the contribution is primarily a new algorithm, the paper should make it clear how to reproduce that algorithm.
  (b) If the contribution is primarily a new model architecture, the paper should describe the architecture clearly and fully.
  (c) If the contribution is a new model (e.g., a large language model), then there should either be a way to access this model for reproducing the results or a way to reproduce the model (e.g., with an open-source dataset or instructions for how to construct the dataset).
  (d) We recognize that reproducibility may be tricky in some cases, in which case authors are welcome to describe the particular way they provide for reproducibility. In the case of closed-source models, it may be that access to the model is limited in some way (e.g., to registered users), but it should be possible for other researchers to have some path to reproducing or verifying the results.

5. **Open access to data and code**

   Question: Does the paper provide open access to the data and code, with sufficient instructions to faithfully reproduce the main experimental results, as described in supplemental material?

   Answer: [Yes]

   Justification: Yes, see `latent-planning.github.io`.

   Guidelines:

   - The answer NA means that paper does not include experiments requiring code.
   - Please see the NeurIPS code and data submission guidelines (`https://nips.cc/public/guides/CodeSubmissionPolicy`) for more details.
   - While we encourage the release of code and data, we understand that this might not be possible, so "No" is an acceptable answer. Papers cannot be rejected simply for not including code, unless this is central to the contribution (e.g., for a new open-source benchmark).
   - The instructions should contain the exact command and environment needed to run to reproduce the results. See the NeurIPS code and data submission guidelines (`https://nips.cc/public/guides/CodeSubmissionPolicy`) for more details.
   - The authors should provide instructions on data access and preparation, including how to access the raw data, preprocessed data, intermediate data, and generated data, etc.
   - The authors should provide scripts to reproduce all experimental results for the new proposed method and baselines. If only a subset of experiments are reproducible, they should state which ones are omitted from the script and why.
   - At submission time, to preserve anonymity, the authors should release anonymized versions (if applicable).

- Providing as much information as possible in supplemental material (appended to the paper) is recommended, but including URLs to data and code is permitted.

6. **Experimental setting/details**

   Question: Does the paper specify all the training and test details (e.g., data splits, hyperparameters, how they were chosen, type of optimizer, etc.) necessary to understand the results?

   Answer: [Yes]

   Justification:

   Guidelines:

   - The answer NA means that the paper does not include experiments.
   - The experimental setting should be presented in the core of the paper to a level of detail that is necessary to appreciate the results and make sense of them.
   - The full details can be provided either with the code, in appendix, or as supplemental material.

7. **Experiment statistical significance**

   Question: Does the paper report error bars suitably and correctly defined or other appropriate information about the statistical significance of the experiments?

   Answer: [Yes]

   Justification: All experiments report standard error. In addition, we conduct tests to verify statistical significance of results.

   Guidelines:

   - The answer NA means that the paper does not include experiments.
   - The authors should answer "Yes" if the results are accompanied by error bars, confidence intervals, or statistical significance tests, at least for the experiments that support the main claims of the paper.
   - The factors of variability that the error bars are capturing should be clearly stated (for example, train/test split, initialization, random drawing of some parameter, or overall run with given experimental conditions).
   - The method for calculating the error bars should be explained (closed form formula, call to a library function, bootstrap, etc.)
   - The assumptions made should be given (e.g., Normally distributed errors).
   - It should be clear whether the error bar is the standard deviation or the standard error of the mean.
   - It is OK to report 1-sigma error bars, but one should state it. The authors should preferably report a 2-sigma error bar than state that they have a 96% CI, if the hypothesis of Normality of errors is not verified.
   - For asymmetric distributions, the authors should be careful not to show in tables or figures symmetric error bars that would yield results that are out of range (e.g. negative error rates).
   - If error bars are reported in tables or plots, The authors should explain in the text how they were calculated and reference the corresponding figures or tables in the text.

8. **Experiments compute resources**

   Question: For each experiment, does the paper provide sufficient information on the computer resources (type of compute workers, memory, time of execution) needed to reproduce the experiments?

   Answer: [Yes]

   Justification:

   Guidelines:

   - The answer NA means that the paper does not include experiments.
   - The paper should indicate the type of compute workers CPU or GPU, internal cluster, or cloud provider, including relevant memory and storage.

- The paper should provide the amount of compute required for each of the individual experimental runs as well as estimate the total compute.
- The paper should disclose whether the full research project required more compute than the experiments reported in the paper (e.g., preliminary or failed experiments that didn't make it into the paper).

9. **Code of ethics**

   Question: Does the research conducted in the paper conform, in every respect, with the NeurIPS Code of Ethics `https://neurips.cc/public/EthicsGuidelines`?

   Answer: [Yes]

   Justification:

   Guidelines:

   - The answer NA means that the authors have not reviewed the NeurIPS Code of Ethics.
   - If the authors answer No, they should explain the special circumstances that require a deviation from the Code of Ethics.
   - The authors should make sure to preserve anonymity (e.g., if there is a special consideration due to laws or regulations in their jurisdiction).

10. **Broader impacts**

    Question: Does the paper discuss both potential positive societal impacts and negative societal impacts of the work performed?

    Answer: [NA]

    Justification: This paper conducts research in the area of optimal control and RL, which do have societal impact. However, this specific research paper does not have substative societal impact.

    Guidelines:

    - The answer NA means that there is no societal impact of the work performed.
    - If the authors answer NA or No, they should explain why their work has no societal impact or why the paper does not address societal impact.
    - Examples of negative societal impacts include potential malicious or unintended uses (e.g., disinformation, generating fake profiles, surveillance), fairness considerations (e.g., deployment of technologies that could make decisions that unfairly impact specific groups), privacy considerations, and security considerations.
    - The conference expects that many papers will be foundational research and not tied to particular applications, let alone deployments. However, if there is a direct path to any negative applications, the authors should point it out. For example, it is legitimate to point out that an improvement in the quality of generative models could be used to generate deepfakes for disinformation. On the other hand, it is not needed to point out that a generic algorithm for optimizing neural networks could enable people to train models that generate Deepfakes faster.
    - The authors should consider possible harms that could arise when the technology is being used as intended and functioning correctly, harms that could arise when the technology is being used as intended but gives incorrect results, and harms following from (intentional or unintentional) misuse of the technology.
    - If there are negative societal impacts, the authors could also discuss possible mitigation strategies (e.g., gated release of models, providing defenses in addition to attacks, mechanisms for monitoring misuse, mechanisms to monitor how a system learns from feedback over time, improving the efficiency and accessibility of ML).

11. **Safeguards**

    Question: Does the paper describe safeguards that have been put in place for responsible release of data or models that have a high risk for misuse (e.g., pretrained language models, image generators, or scraped datasets)?

    Answer: [NA]

    Justification:

Guidelines:

- The answer NA means that the paper poses no such risks.
- Released models that have a high risk for misuse or dual-use should be released with necessary safeguards to allow for controlled use of the model, for example by requiring that users adhere to usage guidelines or restrictions to access the model or implementing safety filters.
- Datasets that have been scraped from the Internet could pose safety risks. The authors should describe how they avoided releasing unsafe images.
- We recognize that providing effective safeguards is challenging, and many papers do not require this, but we encourage authors to take this into account and make a best faith effort.

12. **Licenses for existing assets**

    Question: Are the creators or original owners of assets (e.g., code, data, models), used in the paper, properly credited and are the license and terms of use explicitly mentioned and properly respected?

    Answer: [Yes]

    Justification:

    Guidelines:

    - The answer NA means that the paper does not use existing assets.
    - The authors should cite the original paper that produced the code package or dataset.
    - The authors should state which version of the asset is used and, if possible, include a URL.
    - The name of the license (e.g., CC-BY 4.0) should be included for each asset.
    - For scraped data from a particular source (e.g., website), the copyright and terms of service of that source should be provided.
    - If assets are released, the license, copyright information, and terms of use in the package should be provided. For popular datasets, `paperswithcode.com/datasets` has curated licenses for some datasets. Their licensing guide can help determine the license of a dataset.
    - For existing datasets that are re-packaged, both the original license and the license of the derived asset (if it has changed) should be provided.
    - If this information is not available online, the authors are encouraged to reach out to the asset's creators.

13. **New assets**

    Question: Are new assets introduced in the paper well documented and is the documentation provided alongside the assets?

    Answer: [Yes]

    Justification:

    Guidelines:

    - The answer NA means that the paper does not release new assets.
    - Researchers should communicate the details of the dataset/code/model as part of their submissions via structured templates. This includes details about training, license, limitations, etc.
    - The paper should discuss whether and how consent was obtained from people whose asset is used.
    - At submission time, remember to anonymize your assets (if applicable). You can either create an anonymized URL or include an anonymized zip file.

14. **Crowdsourcing and research with human subjects**

    Question: For crowdsourcing experiments and research with human subjects, does the paper include the full text of instructions given to participants and screenshots, if applicable, as well as details about compensation (if any)?

Answer: [NA]

Justification:

Guidelines:

- The answer NA means that the paper does not involve crowdsourcing nor research with human subjects.
- Including this information in the supplemental material is fine, but if the main contribution of the paper involves human subjects, then as much detail as possible should be included in the main paper.
- According to the NeurIPS Code of Ethics, workers involved in data collection, curation, or other labor should be paid at least the minimum wage in the country of the data collector.

15. **Institutional review board (IRB) approvals or equivalent for research with human subjects**

    Question: Does the paper describe potential risks incurred by study participants, whether such risks were disclosed to the subjects, and whether Institutional Review Board (IRB) approvals (or an equivalent approval/review based on the requirements of your country or institution) were obtained?

    Answer: [NA]

    Justification:

    Guidelines:

    - The answer NA means that the paper does not involve crowdsourcing nor research with human subjects.
    - Depending on the country in which research is conducted, IRB approval (or equivalent) may be required for any human subjects research. If you obtained IRB approval, you should clearly state this in the paper.
    - We recognize that the procedures for this may vary significantly between institutions and locations, and we expect authors to adhere to the NeurIPS Code of Ethics and the guidelines for their institution.
    - For initial submissions, do not include any information that would break anonymity (if applicable), such as the institution conducting the review.

16. **Declaration of LLM usage**

    Question: Does the paper describe the usage of LLMs if it is an important, original, or non-standard component of the core methods in this research? Note that if the LLM is used only for writing, editing, or formatting purposes and does not impact the core methodology, scientific rigorousness, or originality of the research, declaration is not required.

    Answer: [NA]

    Justification:

    Guidelines:

    - The answer NA means that the core method development in this research does not involve LLMs as any important, original, or non-standard components.
    - Please refer to our LLM policy (https://neurips.cc/Conferences/2025/LLM) for what should or should not be described.